

MODELING OF OPTIMAL RECONFIGURABLE
MICROGRID FOR ELECTRIC VEHICLE INTEGRATION

BY

AZRIN BIN SAEDI

A dissertation submitted in fulfillment of the requirement for
the degree of Master of Science (Computer and Information
Engineering).

Kulliyyah of Engineering
International Islamic University Malaysia

FEBRUARY 2023

ABSTRACT

The world is experiencing the impact of climate change, such as rising sea levels, extreme weather, natural disaster, and reduced food production. These issues strongly correlate with the global warming phenomenon caused by high carbon emissions; in fact, the transportation sector is recorded as one of the highest contributors. Therefore, many countries are phasing out internal combustion engine (ICE) usage by replacing them with more environment-friendly electric vehicles (EVs). However, as essential infrastructure in the EV ecosystem, the EV charging station must be installed in huge numbers at various locations. Excessive charging loads could cause challenges to the microgrid, such as harmonic distortion, voltage instability, and high-power losses. As a solution, microgrid reconfiguration modeling is needed. Hence, this research develops an optimum reconfigurable microgrid to minimize power losses and increase voltage stability. The most efficient metaheuristic method, Cuckoo Search Algorithm (CSA) is used to find the best reconfiguration as it is involved with the multi-objectives problem, in comparison to Genetic Algorithm (GA) as the second most efficient metaheuristic method and Particle Swarm Optimization (PSO) as the least most efficient metaheuristic method. The two different scales of bus networks, IEEE-33 bus, and IEEE-69 bus, are utilized as a microgrid test model in various charging conditions. The simulation results show the power losses decreased up to 99.47 %, while the voltage stability index (VSI) value increased up to 6.1386 approximately with integration of EVs load. Moreover, the compared results with GA and PSO algorithm show that the CSA performed better in terms of power loss reduction and voltage stability for all cases.

ملخص البحث

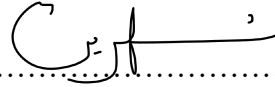
يشهد العالم تأثيرات ناتجة عن تغير المناخ، مثل ارتفاع مستوى سطح البحر، والطقس القاسي، والكوارث الطبيعية، وانخفاض الناتج الغذائي. وترتبط هذه القضايا ارتباطاً وثيقاً بظاهرة الاحتباس الحراري الناجمة عن الانبعاثات العالية للكربون؛ حيث يعدّ قطاع النقل من أكثر المساهمين في هذه الظاهرة. لذلك، تعمل العديد من البلدان على التخلص التدريجي من استخدام محركات الاحتراق الداخلي (ICE) عن طريق الاستعاضة عنها بمركبات كهربائية صديقة للبيئة (EVs). ومع ذلك، فإن محطات شحن المركبات الكهربائية، باعتبارها من ضرورات البنية التحتية للنظام البيئي لهذه المركبات، يتوجب تركيبها بأعداد كبيرة في مواقع متعددة. وبالتالي، فقد تسبب أحمال الشحن الزائدة في حدوث تحديات للشبكة المصغرة، مثل التشوه التوافقي، وعدم استقرار الجهد، وفقدان الطاقة العالية. وكحل هذه المشاكل، هناك حاجة إلى نمذجة إعادة تكوين الشبكة الصغيرة. من هنا، فإن هذا البحث يقترح تطويراً لشبكة مصغرة قابلة لإعادة التكوين بشكل مثالي لتقليل فقد الطاقة وزيادة استقرار الجهد. لقد تم استخدام خوارزمية بحث الوقواق (CSA) باعتبارها الطريقة الأكثر فاعلية في الكشف عن أفضل إعادة تشكيل؛ لأنها تستخدم في حل المسائل متعددة الأهداف، وذلك بالمقارنة مع الخوارزمية الوراثية (GA) كثاني أكثر الطرق كفاءة وفعالية، وكذلك خوارزمية سرب الجسيمات (PSO) باعتبارها طريقة الكشف الأقل كفاءة. كما تم استخدام مقياسين مختلفين لشبكات النقل هما: (IEEE-33 bus)، و (IEEE-69 bus)، كنموذج اختبار للشبكة المصغرة في ظروف شحن مختلفة. وقد أظهرت نتائج المحاكاة أن فقد الطاقة قد انخفض بنسبة تصل إلى 99.47٪، بينما زادت قيمة مؤشر ثبات الجهد (VSI) إلى 6.1386 تقريباً، مع تكامل حمل المركبات الكهربائية. إضافة إلى ذلك، تُظهر نتائج المقارنة مع خوارزميتي

(GA) و (PSO) أن أداء خوارزمية (CSA) كان أفضل من حيث تقليل فقد الطاقة واستقرار الجهد في جميع الحالات.

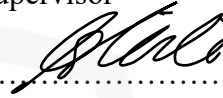


APPROVAL PAGE

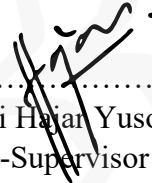
I certify that I have supervised and read this study and that in my opinion, it conforms to acceptable standards of scholarly presentation and is fully adequate, in scope and quality, as a dissertation for the degree of Master of Science (Computer and Information Engineering).



.....
Mohd Shahrin Abu Hanifah
Supervisor



.....
Hilmi Hela Ladin
Co-Supervisor



.....
Siti Hajar Yusoff
Co-Supervisor



.....
Nurul Fadzlın Hasbullah
Co-Supervisor

I certify that I have read this study and that in my opinion it conforms to acceptable standards of scholarly presentation and is fully adequate, in scope and quality, as a dissertation for the degree of Master of Science (Computer and Information Engineering).

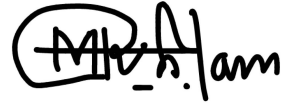


.....
Nur Shahida Binti Midi
Examiner 1



.....
Aisha Hassan Abdalla Hashim
Examiner 2

This dissertation was submitted to the Department of Electrical and Computer Engineering and is accepted as a fulfilment of the requirement for the degree of Master of Electrical and Computer Engineering.



.....
Rafiqul Islam
Head, Department of Electrical and
Computer Engineering

This dissertation was submitted to the Kulliyyah of Engineering and is accepted as a fulfilment of the requirement for the degree of Master of Electrical and Computer Engineering.



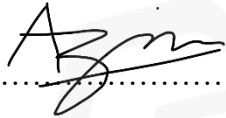
.....
Sany Izan Ihsan
Dean, Kulliyyah of Engineering

DECLARATION

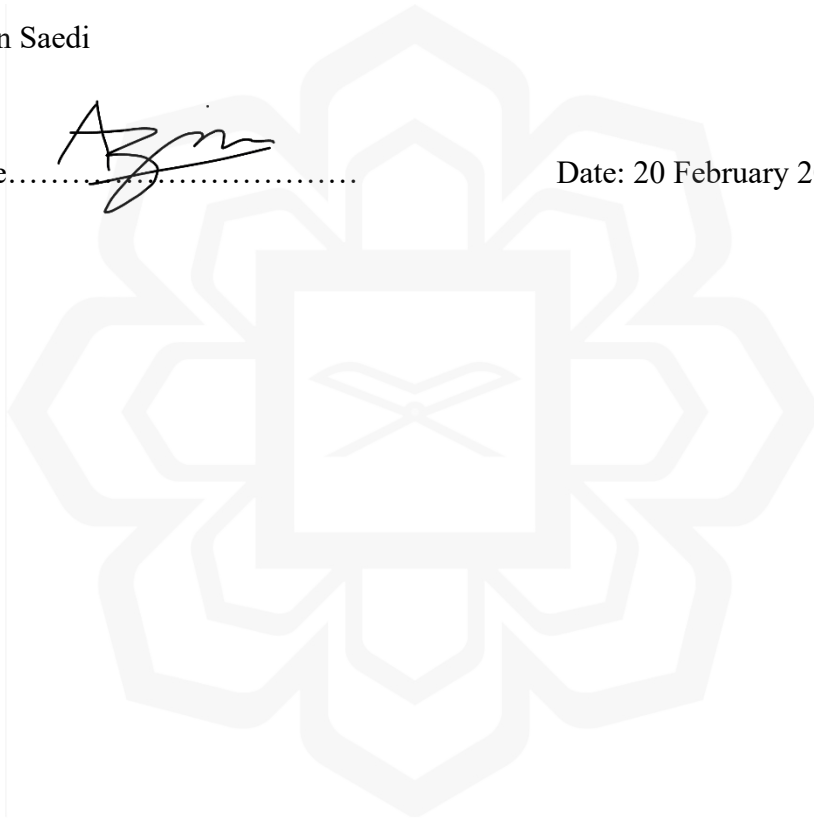
I hereby declare that this dissertation is the result of my own investigations, except where otherwise stated. I also declare that it has not been previously or concurrently submitted as a whole for any other degrees at IIUM or other institutions.

Azrin Bin Saedi

Signature.....



Date: 20 February 2023



INTERNATIONAL ISLAMIC UNIVERSITY MALAYSIA

**DECLARATION OF COPYRIGHT AND AFFIRMATION OF
FAIR USE OF UNPUBLISHED RESEARCH**

**MODELING OF OPTIMAL RECONFIGURABLE
MICROGRID FOR ELECTRIC VEHICLE INTEGRATION**

I declare that the copyright holder of this dissertation is International Islamic University Malaysia.

Copyright © 2022 International Islamic University Malaysia. All rights reserved.

No part of this unpublished research may be reproduced, stored in a retrieval system, or transmitted, in any form or by any means, electronic, mechanical, photocopying, recording or otherwise without prior written permission of the copyright holder except as provided below

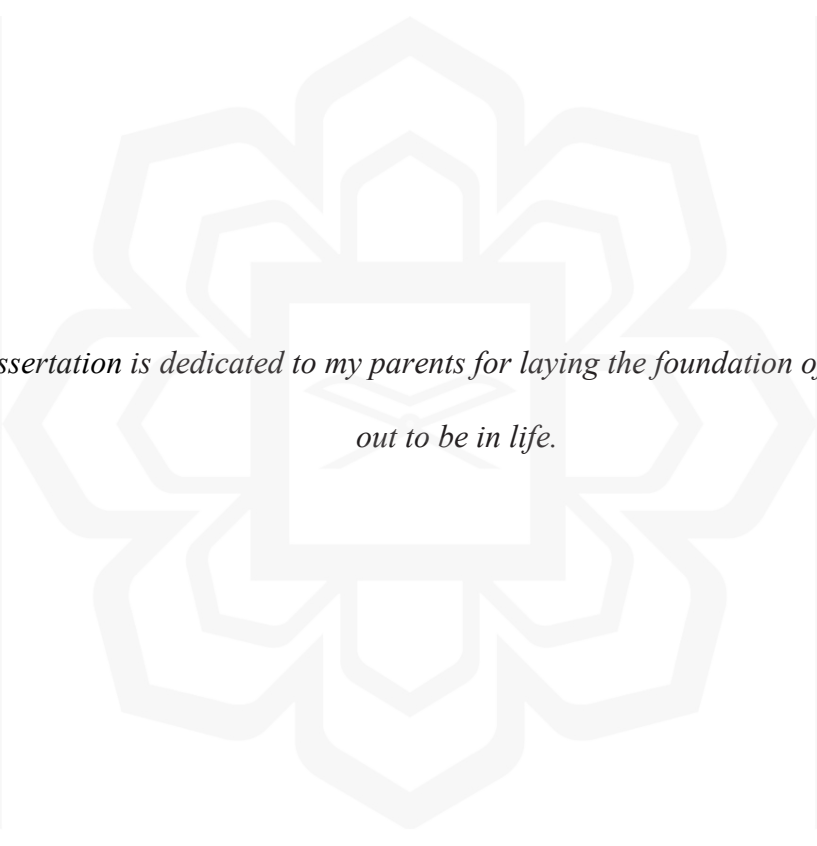
1. Any material contained in or derived from this unpublished research may only be used by others in their writing with due acknowledgement.
2. IIUM or its library will have the right to make and transmit copies (print or electronic) for institutional and academic purpose.
3. The IIUM library will have the right to make, store in a retrieval system and supply copies of this unpublished research if requested by other universities and research libraries.

By signing this form, I acknowledged that I have read and understand the IIUM Intellectual Property Right and Commercialization policy.

Affirmed by Azrin Bin Saedi


.....
Signature

09 March 2023
.....
Date



*This dissertation is dedicated to my parents for laying the foundation of what I turned
out to be in life.*

ACKNOWLEDGEMENTS

All glory is due to Allah, the Almighty, whose Grace and Mercies have been with me throughout the duration of my programme. Although, it has been tasking, His Mercies and Blessings on me ease the herculean task of completing this dissertation.

I am most indebted to by supervisor, Dr Mohd Shahrin Abu Hanifah, whose enduring disposition, kindness, promptitude, thoroughness and friendship have facilitated the successful completion of my work. I put on record and appreciate his detailed comments, useful suggestions and inspiring queries which have considerably improved this dissertation. His brilliant grasp of the aim and content of this work led to his insightful comments, suggestions and queries which helped me a great deal. Despite his commitments, he took time to listen and attend to me whenever requested. The moral support he extended to me is in no doubt a boost that helped in building and writing the draft of this research work. I am also grateful to my co-supervisors, Dr. Hilmi Hela Ladin, Assoc. Prof. Dr. Siti Hajar Yusoff and Prof. Dr. Nurul Fadzlin Hasbullah whose support and cooperation contributed to the outcome of this work.

Lastly, my gratitude goes to my beloved parents; for their prayers, understanding and endurance while away.

Once again, we glorify Allah for His endless mercy on us one of which is enabling us to successfully round off the efforts of writing this dissertation. Alhamdulillah.

TABLE OF CONTENTS

Abstract	ii
Abstract in Arabic	iii
Approval Page.....	v
Declaration	vii
Copyright	viii
Dedication	ix
Acknowledgements	x
Table Of Contents	xi
List Of Tables	xiii
List Of Figures	xv
List Of Symbols	xvii
CHAPTER ONE: INTRODUCTION	1
1.1 Overview.....	1
1.2 Problem Statement.....	2
1.3 Research Hypothesis.....	3
1.4 Research Objectives.....	3
1.5 Research Methodologies.....	3
1.6 Research Scope	5
1.7 Dissertation Organisation	5
CHAPTER TWO: LITERATURE REVIEW.....	6
2.1 Overview	6
2.2 Microgrid	7
2.2.1 AC Microgrid.....	9
2.2.2 DC Microgrid.....	10
2.2.3 Hybrid Microgrid	11
2.3 Loss Minimisation Technique.....	12
2.3.1 Distributed Generations Allocation	12
2.3.2 Capacitor Allocation	13
2.3.3 Network Reconfiguration.....	14
2.4 Electric Vehicle Chargers	15
2.4.1 Slow Chargers	17
2.4.2 Fast Chargers	17
2.5 Voltage Stability	18
2.5.1 Line VSI.....	19
2.5.2 Bus VSI.....	20
2.6 Optimisation Algorithm	20
2.6.1 Genetic Algorithm	21
2.6.2 Particle Swarm Optimisation.....	23
2.6.3 Cuckoo Search Algorithm.....	24
2.7 Related Works.....	29

2.8 Summary	32
CHAPTER THREE: RESEARCH METHODOLOGY	33
3.1 Overview	33
3.2 Power Flow	33
3.2.1 Power Flow Formulation	33
3.2.2 Power Flow Equation and Admittance Matrix	36
3.2.3 Newton-Raphson Technique.....	39
3.3 IEEE Bus System.....	42
3.3.1 IEEE-33 Bus System.....	42
3.3.2 IEEE-69 Bus System.....	47
3.4 Objective Functions	53
3.4.1 Power Loss.....	53
3.4.2 Voltage Stability Index	54
3.4.3 Power Loss And Voltage Stability Index.....	55
3.5 Cuckoo Search Algorithm.....	55
3.6 Summary	59
CHAPTER FOUR: RESULTS AND DISCUSSIONS.....	60
4.1 Overview	60
4.2 IEEE-33 Bus System.....	60
4.2.1 Without EV Charging Load (Index 0)	61
4.2.2 Index 1 in IEEE-33 Bus System	62
4.2.3 Index 2 in IEEE-33 Bus System	64
4.2.4 Index 3 in IEEE-33 Bus System	66
4.2.5 Index 4 in IEEE-33 Bus System	68
4.2.6 Index 5 in IEEE-33 Bus System	70
4.2.7 Index 6 in IEEE-33 Bus System	71
4.2.8 Analysis of PSO, GA, and CSA in IEEE-33 Bus System	73
4.3 IEEE-69 Bus System.....	77
4.3.1 Without EV Charging Load (Index 0)	77
4.3.2 Index 1 in IEEE-69 Bus System	79
4.3.3 Index 2 in IEEE-69 Bus System	81
4.3.4 Index 3 in IEEE-69 Bus System	83
4.3.5 Index 4 in IEEE-69 Bus System	85
4.3.6 Index 5 in IEEE-69 Bus System	87
4.3.7 Index 6 in IEEE-69 Bus System	89
4.3.8 Analysis of PSO, GA, and CSA in IEEE-69 Bus System	91
4.4 Summary	94
CHAPTER FIVE: CONCLUSION	95
5.1 Conclusion	95
5.2 Limitations And Future Work.....	97
REFERENCES.....	98

LIST OF TABLES

Table 2.1	Charging Modes of IEC 61851-1 (Triviño et al., 2021)	16
Table 2.2	Charging modes of SAE J1772 Standard (Kongjeen & Bhumkittipich, 2018)	17
Table 2.3	Metaheuristic Algorithms Classification (Wong & Ming, 2019)	21
Table 2.4	Comparison of GA and CSA (Yang & Deb, 2009)	28
Table 2.5	Comparison of PSO and CS (Yang & Deb, 2009)	28
Table 2.6	Table of Related Works	30
Table 3.1	Bus type in power flow problem (Albadi, 2020)	35
Table 3.2	Data of IEEE-33 bus system	43
Table 3.3	Fundamental Loop of IEEE-33 bus system	44
Table 3.4	Index cases of IEEE-33 bus system (Deb, Tammi, et al., 2018)	46
Table 3.5	Data of IEEE-69 bus system	48
Table 3.6	Fundamental Loop of the IEEE-69 bus system	51
Table 3.7	Index cases of the IEEE-69 bus system	52
Table 4.1	IEEE-33 for CSA Index 0	61
Table 4.2	IEEE-33 for CSA Index 1	63
Table 4.3	IEEE-33 for CSA Index 2	65
Table 4.4	IEEE-33 for CSA Index 3	67
Table 4.5	IEEE-33 for CSA Index 4	68
Table 4.6	IEEE-33 for CSA Index 5	70
Table 4.7	IEEE-33 for CSA Index 6	72
Table 4.8	IEEE-69 for CSA Index 0	78
Table 4.9	IEEE-69 for CSA Index 1	80
Table 4.10	IEEE-69 for CSA Index 2	82
Table 4.11	IEEE-69 for CSA Index 3	84

Table 4.12	IEEE-69 for CSA Index 4	86
Table 4.13	IEEE-69 for CSA Index 5	88
Table 4.14	IEEE-69 for CSA Index 6	90



LIST OF FIGURES

Figure 2.1	AC Microgrid structure (Meje et al., 2020)	9
Figure 2.2	DC microgrid structure (Meje et al., 2020)	10
Figure 2.3	Hybrid Microgrid structure (Pan et al., 2018)	11
Figure 2.4	IEEE-33 bus system with battery energy storages and DGs (Abdolahi et al., 2018)	13
Figure 2.5	Representation of two buses in a power system (Modarresi et al., 2016)	19
Figure 2.6	General GA pseudocode (Immanuel & Chakraborty, 2019)	22
Figure 2.7	GA Flow Chart (Immanuel & Chakraborty, 2019)	23
Figure 2.8	General steps of PSO (Ülker & Ülker, 2018)	24
Figure 2.9	Pseudocode of CSA via Levy Flights (Yang & Deb, 2009)	26
Figure 2.10	Levy Flight Path simulation in 2-D Plane (Ali et al., 2021)	27
Figure 3.1	Flow of current to load bus (Albadi, 2020)	37
Figure 3.2	IEEE-33 initial configuration	45
Figure 3.3	Index 1 of IEEE-33 bus system (1500 kW at bus 2)	47
Figure 3.4	IEEE-69 initial reconfiguration (Nguyen et al., 2016)	48
Figure 3.5	Index 1 of IEEE-69 bus system (1500 kW at bus 2)	53
Figure 3.6	Flowchart of microgrid reconfiguration by using CSA via Levy Flight.	58
Figure 4.1	Comparison of power losses obtained by CSA, PSO, and GA for all cases in the IEEE-33 bus system	75
Figure 4.2	Comparison of VSI obtained by CSA, PSO, and GA for all cases in the IEEE-33 bus system	76
Figure 4.3	Comparison of objective function score between CSA, PSO, and GA for all cases in the IEEE-33 bus system	77
Figure 4.4	Comparison of power loss obtained between CSA, PSO, and GA for all cases in the IEEE-69 bus system	92

Figure 4.5	Comparison of VSI between CSA, PSO, and GA for all cases in the IEEE-69 bus system	93
Figure 4.6	Comparison of objective function score between CSA, PSO, and GA for all cases in the IEEE-69 bus system	94



LIST OF SYMBOLS

α	Step size
c_1	Cognitive parameter
c_2	Social parameter
G_{best}	Global best
I_i	Current flow into the bus (A)
l_a	Upper bound
l_b	Lower bound
N	Iteration number
n	Number of nest
n_d	Nest dimension
n_e	Tie switch dimension
P_{best}	Particle best
P_i	Real power (W)
P_{loss}	Power loss (W)
p_a	Discoverability probability
Q_i	Reactive power (VAR)
R	Resistance (Ω)
S_i	Apparent power (VA)
V_i	Current Bus voltage (V)
V_j	Neighbor bus voltage (V)
v_i	Velocity
w	Inertia
X	Reactance (Ω)
x	Open switch set
y_{ij}	Admittance between current bus and neighboring bus (S)

CHAPTER ONE

INTRODUCTION

1.1 OVERVIEW

The internal combustion engine (ICE) has been widely used in the automotive industry and has continuously developed since the 19th century. Modern ICEs use fossil fuels efficiently compared to older version of the ICEs. However, ICEs still use fossil fuels to generate energy to move vehicles. Fossil fuel combustion releases carbon dioxide into the air and makes detrimental to the environment. Carbon dioxides cause the effect of global warming as the gas trap heat in the atmosphere and increase the earth's surface and ocean temperature. Consequently, sea-level increases and more unstable weather are expected to occur frequently. Sea levels are expected to increase up to 30 cm to 65 cm by 2050 (Horton et al., 2005).

Fortunately, carbon dioxide reduction efforts have been encouraged worldwide since the 2000s. Most prominently, United Nations Framework Convention on Climate Change was established by United Nations as an effort to mitigate the effect of global warming. Paris Agreement was signed by 196 parties that aim to limit global warming to 2 °C below pre-industrial levels and try to take considerable action to limit temperature increase 1.5 °C below pre-industrial levels (Gao et al., 2017). Thus, one main effort of carbon dioxide emission reduction is the introduction of Electric Vehicles (EVs). EVs are considered one way to limit carbon dioxide emissions because the focus on renewable energy implementation is increasing to reduce electricity generation dependency on fossil fuels.

In EV operation, EV uses one or more electric engines or traction engines for vehicle driving. EVs are powered by electricity supplied from an energy storage device like a battery or large-scale capacitor. As the storage needs to be charged using a power outlet beforehand, numerous charging stations with the interconnection to electric grids need to be deployed strategically. Thus, it is one of the most critical infrastructures in meeting the increasing number of EVs on the road. Meanwhile, in Malaysia, one target of National Automotive Policy 2020 (NAP 2020) is Malaysia will develop EV Smart Grid Interoperability Center by 2030 (*Kementerian Perdagangan Antarabangsa Dan Industri*, n.d.). Currently, there are more than 200 public EV charging stations in peninsular Malaysia, and it is expected to accommodate 125,000 units by 2030.

1.2 PROBLEM STATEMENT

In meeting the rising number of EVs, arguably, one of the most crucial infrastructures is to have sufficient charging stations. Consequently, these charging stations are mostly connected to the power grid. Hence, those charging activities cause some negative impact on the grid. For instance, the uncoordinated charging of EVs degrades voltage profile (Rahman et al., 2022), increases peak load (Park, 2018), cause harmonic distortions (Ahmed et al., 2021), increases power losses (Deb, Kalita, et al., 2018), and equipment overloading. With these problems, the grid's reliability was being questioned. Thus, this research is aimed to utilize a reconfigurable microgrid to mitigate the impact of EV charging load on the network.

1.3 RESEARCH HYPOTHESIS

A reconfigurable microgrid can reduce power loss and increase voltage stability by finding the best path to deliver power, thus a model of a reconfigurable microgrid was needed to apply on small-scale and medium-scale microgrids. The solution of the reconfiguration is optimized as the result of the simulation is the least power loss and best voltage stability. But, to find the best solution, an algorithm was needed. It is expected that Cuckoo Search Algorithm (CSA) is a better algorithm to find the solution for reconfigurable microgrids compared with the Particle Swarm Optimization (PSO) and Genetic Algorithm (GA).

1.4 RESEARCH OBJECTIVES

- i. To assess the impact of EV charging load on the microgrid.
- ii. To develop an optimum reconfigurable microgrid for minimizing the power losses and increasing voltage stability by using CSA, PSO, and GA with EV charging loads integration.
- iii. To apply the developed model/algorithm to small scale and medium scale microgrids.

1.5 RESEARCH METHODOLOGIES

The first step to achieve research objective is assessment of the EV charging load on the microgrid. Thus, a comprehensive review of EV charging load impact on the microgrid was needed. Then, a standard IEEE-33 bus test system was used as a microgrid model. Power

flow calculation was being performed using MATPOWER 6.0 toolbox in MATLAB under both conditions with and without EV charging load, respectively. The impact of EV charging loads on the microgrid was analyzed especially in terms of power loss and voltage stability. From here, objective number 1 which is to assess the impact of EV charging load on microgrids was achieved.

The second step to achieve research objectives is modeling of reconfigurable microgrid with the interconnection of EV. Thus, a reconfigurable microgrid model of the IEEE-33 bus test system with the integration of EV was formulated in a MATLAB software environment. Data of the IEEE-33 bus system which is real power and reactive power of busloads and resistance and reactance of bus system lines was loaded in the MATLAB software. The number of EV charging stations was increased as well as the charging load size and installed location was varied. Power flow calculation of the system was executed by using MATPOWER 6.0 toolbox to ensure the reliability of the system models.

The third step to achieve research objective is developing the optimum model. Thus, the result was analyzed by using a CSA and the parameters was varied to get optimum fitness function. The process was repeated until the minimum power loss and highest voltage stability are achieved. The result was compared using a GA and PSO. From here, objective 2 which is to develop an optimum reconfigurable microgrid model for minimizing the power losses and increasing voltage stability by using CSA was achieved.

Finally, to achieve research objectives is by applying optimum model on medium scale microgrid. The step is the result was validated by using medium scale test model which has a larger number of load bus which is IEEE-69 bus system with respect of IEEE-69 bus system data. From here, objective 3 which is to apply on small scale and medium scale microgrid was achieved.

1.6 RESEARCH SCOPE

The research scope of the research is microgrid. Thus, wide area synchronous grid and super grid are not in this research scope. In terms of power generations and loads, only the effect of the EV charger on the power distribution network is within the research scope and the effect of the distribution generator is not within research scope. Finally, the algorithm application is CSA in comparison with the PSO and GA. Other algorithms are not within the research scope.

1.7 DISSERTATION ORGANISATION

This dissertation contains five chapters. The organization of this dissertation is Chapter 1: Introduction, Chapter 2: Literature Review, Chapter 3: Methodology, Chapter 4: Result and Discussion, and Chapter 5: Conclusion.

In Chapter 1, introduction of overall dissertation was explained. This includes problem statement, research hypothesis, research objectives, research methodologies, research scope and dissertation organization. Meanwhile, Chapter 2 contains literature review of this dissertation. This chapter explains overview of literature reviews, microgrids, loss minimization technique, electric vehicle chargers, voltage stability, optimization algorithm and related works. Chapter 3 is the methodologies of this dissertation. Power flow formulation and techniques, IEEE bus system, objective functions and cuckoo search algorithm was explained here. Chapter 4 is the result and discussion of this dissertation. The result was divided between IEEE-33 bus system and IEEE-69 bus system. Chapter 5 is the conclusion and limitation of this dissertation.

CHAPTER TWO

LITERATURE REVIEW

2.1 OVERVIEW

Microgrid is the main subject of this research. In the microgrid system, EV charging loads was integrated into microgrid at different buses. The microgrid can be reconfigurable by using CSA and the optimal configuration was found based on the minimum power loss and the most stable Voltage Stability Index (VSI) as the best result. The design to find the best solution is the model of this dissertation. The literature review covers elements of this research and views of other researchers about those elements. Literature review also covers related works of other researchers and their findings. The elements of this research are microgrid type, loss minimization techniques, EV charger types, VSI and optimization algorithm. Microgrid is divided between AC, DC, and hybrid. Loss minimization techniques cover between distributed generations allocation, capacitor allocation and network reconfiguration. EV charger types covered are slow chargers and fast chargers. VSI are categorized between line VSI, bus VSI, and overall VSI. Optimization algorithms covered are GA, PSO and CSA and other algorithms are not covered.

EVs are seen as the better solution to combat climate change and global warming due to the alternative of ICE vehicles as EVs use electricity as opposed to fuel burning. The transition from ICE vehicles to EVs has many economic and environmental benefits. However, as EVs number increase, the charging demands also increase (Deb, Tammi, et al., 2018). Thus, EV implementation and integration can cause an extra burden on the existing power grid. In other words, as shown by many researchers, EV charging loads can cause harmonic distortion (Barrero-González et al., 2019; Jiang et al., 2014; Nikitha et al., 2018), increase peak load (Arango Castellanos et al., 2019; Di Silvestre et al., 2013; Fan et

al., 2013; Sehar et al., 2017), and decrease voltage profile (Dharmakeerthi et al., 2014; Zhang et al., 2016; Zhou et al., 2016). A. Ul-Haq et al. find that 60% EV penetration causes a 109% power consumption increase (Ul-Haq et al., 2015). In a study of EV penetration to North Ireland power system, only one region can support 7kW, 22kW, and 50kW, two regions can support 7kW and 22kW rating charging, eight regions can support 7kW charging and the other 12 regions cannot support any EV charging load (Zhou et al., 2016). Besides that, magnetic devices in the power system can be degraded by total harmonic distortion presented in the system, meanwhile, EV charging load also can cause total harmonic distortion (Nikitha et al., 2018). In a study by F. Barrero-González et al., EV charging station load can cause up to 26% of total harmonic distortion (Barrero-González et al., 2019).

2.2 MICROGRID

The microgrid was studied as an effort to combat dependency on fossil fuels due to environmental concerns and to achieve Sustainable Development Goals (Kumar et al., 2019). In comparison with a conventional power plant, microgrid offers renewable energy usage as power generation thus making microgrid technology more eco-friendly compared to the conventional power plant. Besides that, microgrids also may increase power system reliability, reduce network congestion, and reduce transmission power loss (Zaki Diab et al., 2019). Microgrids also can be working as autonomous networks or non-autonomously. Autonomous microgrids are microgrid networks disconnected from the power grid, meanwhile non-autonomous microgrids are interconnected with the power grid. Thus, off-grid microgrids can provide power to isolated areas like an island. But there are a few challenges to operating off-grid microgrids such as stability and load management due to their nature isolated from the main grid (Yoldaş et al., 2017).

A microgrid can be divided into three types depending on the technologies used which are AC microgrids, DC microgrids, and Hybrid microgrids. AC microgrids are the dominant technologies used currently as AC power systems used widely in industries since the end of the 19th century. There are a few disadvantages of individual AC microgrids which are low efficiency as AC microgrids require multiple conversions, need reactive power, and have problems with stability and synchronization.

Another type of microgrid technology is the DC microgrid. This technology utilizes DC as the type of electric current. As more energy sources are coming from DC electric current like photovoltaic, DC microgrid is potentially more cost-effective compared to its AC counterpart. DC also only requires a single DC-to-DC conversion to DC loads like many home appliances and off-grid EV charging load stations. Compared to AC, DC has the advantages of no reactive power and no synchronization needed. But the common electricity current type in the industry and residential areas is AC electricity current. To use a DC microgrid for AC loads, DC-to-AC conversion is needed.

The better solution to cater to the problems in AC and DC microgrids is by implementing a hybrid microgrid that uses both AC and DC electric current. In a hybrid microgrid, AC and DC renewable power sources and AC and DC loads are integrated into one microgrid system, thus reducing conversion power losses. The hybrid microgrid is also more appealing AC grids are more common, but DC renewable power sources are more attractive in distributed renewable energy generation. But, as AC is more common in the usage of electrical power transfer in the world, this research focus on AC microgrid. The microgrid simulation in this research is taking account the AC current in the microgrid.

2.2.1 AC Microgrid

In an AC microgrid, power generation, power storage, and loads are connected to an AC bus. As many renewable energy sources are generating DC electric current, AC-to-DC inverters are needed to supply the power into the AC microgrid, thus generating power losses. To connect to DC loads, an AC-to-DC rectifier is needed meanwhile AC-to-AC converter is needed for AC loads. Multiple conversions from DC to AC and back to DC for DC loads decrease the reliability and efficiency of AC microgrids (Meje et al., 2020). Figure 2.1 shows the structure of the AC microgrid.

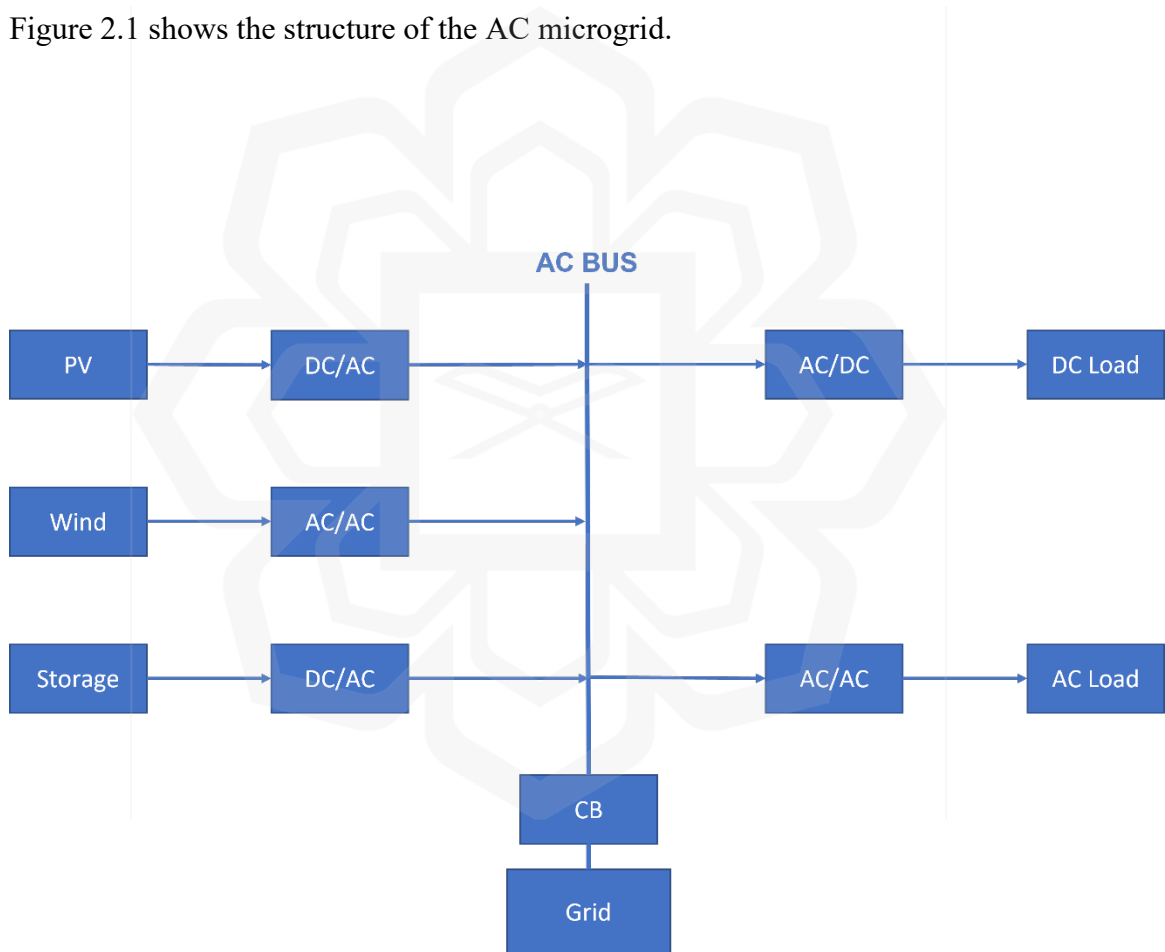


Figure 2.1: AC Microgrid structure (Meje et al., 2020)

2.2.2 DC Microgrid

As many renewable energy sources are in the form of DC electricity type, DC was seen as a better microgrid compared to AC microgrid. Besides that, many electrical loads and energy storage are in the form of DC electricity. DC also needs less power conversion compared to AC microgrids. Thus, DC microgrid can have better efficiency and reliability compared to AC microgrid (Meje et al., 2020). Figure 2.2 shows the DC microgrid structure.

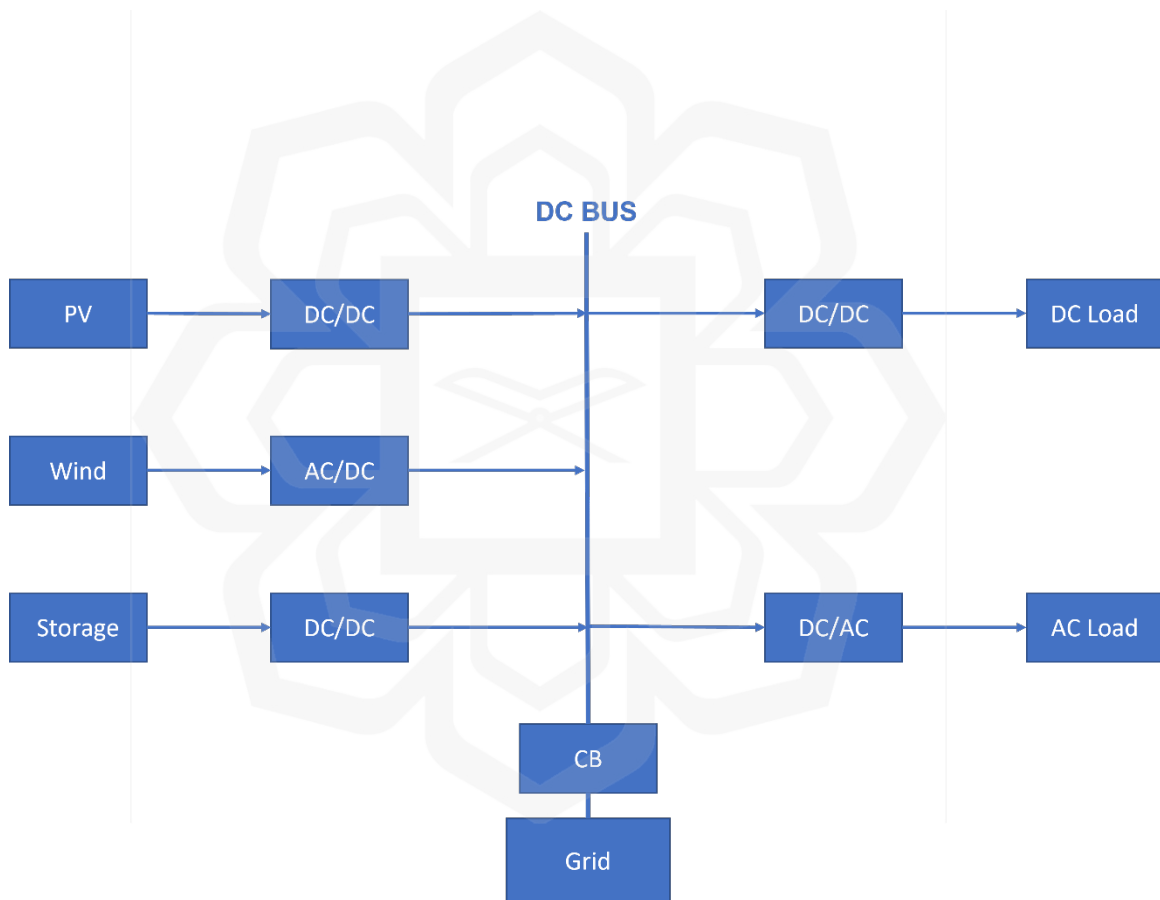


Figure 2.2: DC microgrid structure (Meje et al., 2020)

2.2.3 Hybrid Microgrid

The idea of the hybrid microgrid is to utilize both advantages of the AC and DC microgrid. A hybrid microgrid skips multiple conversions of AC and DC to supply power to the load. This can prevent huge power loss in the overall microgrid system. Besides that, it is also much easier to connect various AC and DC renewable energy sources to the microgrid to minimize conversion loss. A microgrid is considered a controlled power system unit for utility purposes. Compared to conventional micro generation, microgrids cause fewer problems to the utility network. Loads are also coordinated intelligently and properly (Meje et al., 2020). Figure 2.3 shows the structure of hybrid microgrid structure.

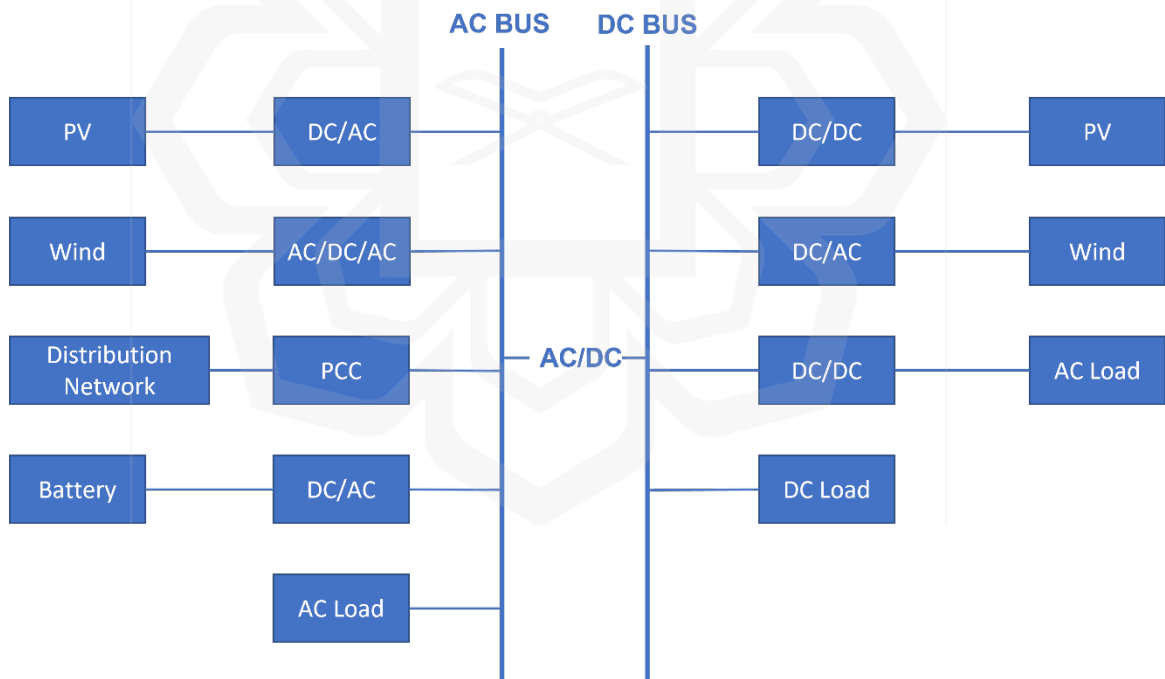


Figure 2.3: Hybrid Microgrid structure (Pan et al., 2018)

2.3 LOSS MINIMISATION TECHNIQUE

Transmission and distribution power loss is perceived as the major concern in power systems. Any losses in the distribution stage become a big issue as electricity demand increases, constraints due to the environment, and the competitive energy market cause transmission and distribution systems to work in overloaded conditions. A load entity system must accept only a power quality and in parallel to get the most benefit of economic cost-effectiveness, researchers are discovering power loss minimization techniques and the best operation practices. Thus, researchers focus on power loss reduction and voltage stability improvement in a power system (Sambaiah & Jayabarathi, 2020). A few methods are suggested for power loss reduction: distributed generations (DGs) allocation, capacitor allocation, and network reconfiguration.

2.3.1 Distributed Generations Allocation

DGs can be defined as “Power generated from supply and demand resources that are significantly less than centralized power generation that distributed throughout distribution power system to meet the energy demand of customer in the system”. Generally, DGs are located near load nodes or the utility side of the meter (Sambaiah & Jayabarathi, 2020).

The main aspect of DG penetrations into a distribution system is the technical, economic, and environmental impact. The implementation of DGs is increasing year by year and the implementation shifts the grid away from traditional centralized power distribution. Thus, the location and appropriate size of DGs are needed to be considered

appropriate to optimize DG allocation benefits (Sambaiah & Jayabarathi, 2020). Figure 2.4 shows DG allocations in a IEEE-33 bus system with battery energy storage.

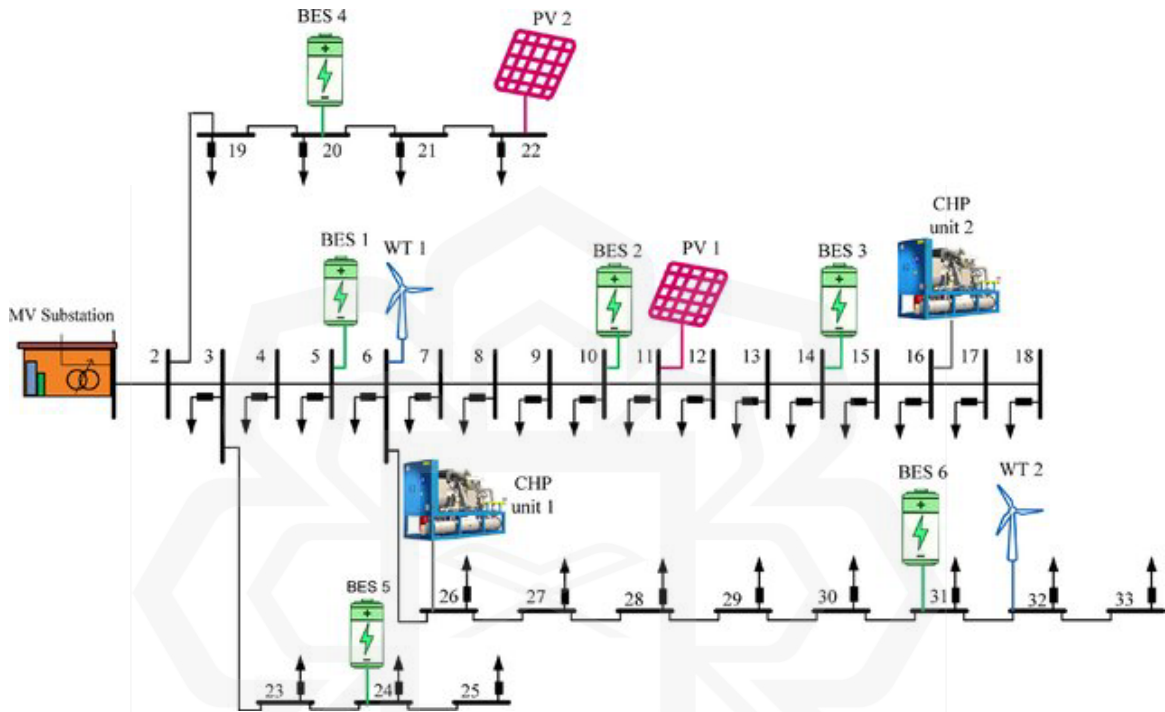


Figure 2.4: IEEE-33 bus system with battery energy storages and DGs (Abdolahi et al., 2018)

2.3.2 Capacitor Allocation

A capacitor can reduce power loss in a power distribution system by the shunt capacitor integration in the system. Capacitors can reduce inductive reactance as the capacitor provides a reactive power source. Originally, researchers conduct their study for voltage control and consequently for power loss reduction. The problems of capacitor allocation

are the suitable unit for the capacitor to be used, the location to install the capacitors, and capacitor sizing to achieve power loss reduction, power factor control, and voltage regulation improvement (Sambaiah & Jayabarathi, 2020).

But there are many benefits of capacitor allocation in a power distribution system. The benefits are energy loss reduction, a decrease in power loss, voltage stability enhancement, handles voltage profile, power flow control, and correction of power factor. Capacitor allocation also can be used in high voltage distribution network systems (Sambaiah & Jayabarathi, 2020).

2.3.3 Network Reconfiguration

Network reconfiguration, also known only as reconfiguration, is the change of topology by switching on or off certain switches in a network, effectively changing the network into a meshed network or radial network. Reconfiguration is essential to decrease power loss. In the primary distribution system, there two switches type existed in the system, which are tie switches and sectionalizing switches. A tie switch is also known as an open switch meanwhile sectionalizing switch is also known as a closed switch. The operation involves alternating change sectionalizing switches and tie switches in the distribution system simultaneously. Effectively change the topology of the current distribution network configuration (Sambaiah & Jayabarathi, 2020).

In this research, to cater to the problem of stability and load management in microgrid, reconfiguration of microgrids is needed to reduce power loss and improve voltage stability. Reconfiguration is needed to maximize voltage profile to all nodes of the distribution network, besides that the general target is to improve load balancing and reduce

power loss (Yoldaş et al., 2017). The objective of reconfiguration in this research is power loss reduction and voltage stability improvement.

There are many advantages of network reconfiguration, such as service restoration in case of feeder faults, bus voltage enhancement, reduce network overload, outage planning for network maintenance, and power loss reduction. Switching operation is the basic in network reconfiguration but the operation is complex due to the many nodes of switching operation and the discrete nature of the switch. Thus, many studies are solving this problem through the heuristic method. Generally, reconfiguration can be solved by using the algorithm by two methods, branch exchange, and loop cutting. Branch exchange is an algorithm that opens and closes switches in pairs to find a feasible radial reconfiguration meanwhile loop cutting is to explore the nodes to be opened in a mesh system (Sambaiah & Jayabarathi, 2020).

In this research, the method used for power loss minimization and voltage stability improvement is by using network reconfiguration by CSA as optimization algorithm. Reconfiguration is chosen as the method to reduce power loss and improve voltage stability as there is no need for additional equipment and power sources like capacitors and DGs. Thus, reconfiguration is simpler, and cost less compared to adding additional equipment in microgrid.

2.4 ELECTRIC VEHICLE CHARGERS

EV energy refill can be operated in two methods: battery swapping and conductive charging. Conductive charging itself can be divided as two types, which are on-board and off-board types (Chen & Liao, 2013). On-board charging limits the power charged into the

vehicle as there are weight, cost, and space constraints in the vehicle. Off-board chargers are not restricted by space and weight (Yilmaz & Krein, 2012). Generally, EV chargers can be divided into two types: slow chargers and fast chargers (FC). (L. Wang et al., 2021). Standardization of charging modes is defined in IEC 61851-1 and SAE J1772 based on power level and input current (AC or DC) (L. Wang et al., 2021). Table 2.1 shows IEC 61851-1 charging modes, meanwhile Table 2.2 shows SAE J1772 Standard charging modes.

Table 2.1: Charging Modes of IEC 61851-1 (Triviño et al., 2021)

Charging Mode	Charging Type	Max. Current (A)	Max. Power (kW)	Charging Time for 50kWh	Distance for a 15 min Charge (km)
Mode 1	Slow	16 A, AC, Single-Phase	3.7	14 h	5
Mode 2	Fast	32 A, AC, Single-Phase	7.4	7 h	9
		32 A, AC, Three-Phase	22	> 2 h	27
Mode 3	Rapid	62 A, AC, Three-Phase	43	> 1 h	54
Mode 4	Ultra-Rapid	400 A, DC	200	15 min	250

Table 2.2: Charging modes of SAE J1772 Standard (Kongjeen & Bhumkittipich, 2018)

Charging Mode	Grid Connection	Voltage (V)	Current (A)	Type of Charge
AC level 1	1 phase	120	12-16	Slow
AC level 2	1 phase	240	<80	Slow
AC level 3	1, 3 phase(s)	240	>80	Slow
DC level 1	-	200-450	80	Slow
DC level 2	-	200-450	200	Medium
DC level 3	-	200-600	400	Fast

2.4.1 Slow Chargers

Slow chargers typically are EV charging load that is lower than the maximum power consumption of a household. It is usually installed at homes and public destinations. The maximum power consumption of a household is 19kW in the United States of America and 22kW in European Union (L. Wang et al., 2021). From the perspective of IEC 61851-1 standard, Mode 1, Mode 2, and Mode 3 are considered slow charging and from the perspective of SAE J1772 Standard, AC level 1 to AC level 3 and DC level 1 are considered slow charging for EV.

2.4.2 Fast Chargers

Meanwhile, fast chargers have a higher power rating than normal household consumption. Typically, fast chargers were installed at fast-charging stations (L. Wang et al., 2021). From the perspective of the IEC 61851-1 standard, Mode 4 is considered fast charging and from

the perspective of SAE J1772 Standard, DC level 1 and level 2 are considered fast charging for EVs.

In this research, the implementation of the charging load station is considering fast charging of around 50kW per vehicle (considering Mode 3 of IEC 61851-1 standard and DC level 2 of SAE J1772 Standard) and 1500 kW for each charging station. Thus, a charging station can cater to up to 30 vehicles at one time.

2.5 VOLTAGE STABILITY

Many blackouts in the world have been caused by voltage instability even though it is a local phenomenon. In studies between 1965 and 2005, in the investigation of 12 cases of blackouts, seven cases in implies that voltage instability is the major cause. Voltage stability is the capability of a power system to sustain stable voltage in case there is additional load admittance, which causes load power increases. Reactive power source failure to supply reactive power or power line failure to deliver required reactive power is the cause of voltage instability.

Voltage stability indices (VSIs) can be divided into three groups, which are line VSIs, bus VSIs, and overall VSIs. Line VSIs are indices that measure the capability of power lines to deliver the required voltage to the load point. Meanwhile, bus stability indices measure whether there is voltage collapse at any bus in the power system. Overall voltage stability measures the overall voltage stability system situation. VSI is measured by calculating all buses or lines of the system and the VSI value is taken from the nearest bus or line to voltage collapse or instability. In overall VSIs, the index can only predict the point of a system collapse. Overall VSIs are not measuring any weak lines or buses

(Modarresi et al., 2016). As this research need to identify which bus is weak and strong, thus this VSI is not considered to be applied in this research. Meanwhile, Danish et al. (2019) divided system parameters or variable-based VSI into only bus VSI and line VSI.

2.5.1 Line VSI

In line VSIs, the discriminant of the voltage quadratic equation must be greater or equal to zero to reach stability. Line VSIs were referred to as a line between two buses in a power system as figured in Figure 2.5 where shunt admittance is neglected. Thus, many line VSI's theoretical base are the same with the assumption make the difference among line VSIs (Modarresi et al., 2016).

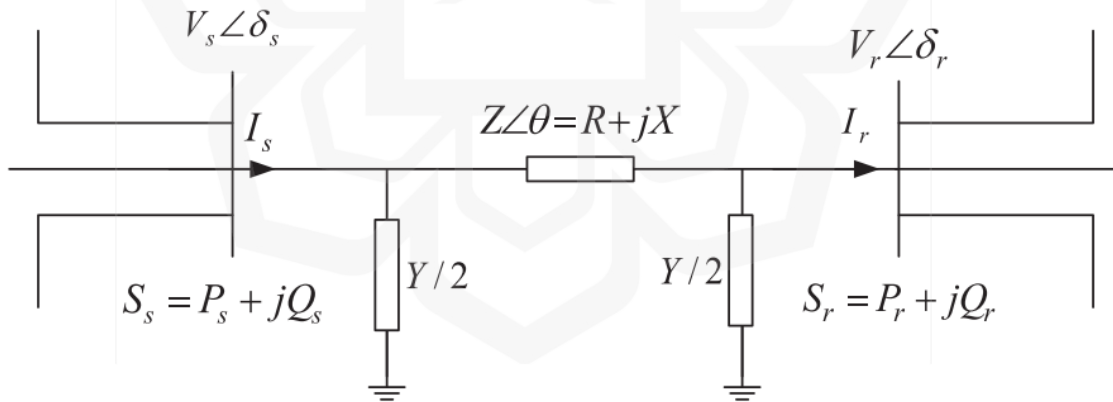


Figure 2.5: Representation of two buses in a power system (Modarresi et al., 2016)

2.5.2 Bus VSI

In bus VSIs, voltage stability is focused on the system buses and the information of weak elements in the power system with potential voltage problems is not provided. Thus, bus VSI cannot be applied to determine a weak power system facility (Modarresi et al., 2016). But, in this research, strength of a bus must be determined EV charging loads are directly connected to a bus in microgrid. If a bus collapse, the power supplied to EV charging load station is halted or not enough and it was affecting the voltage stability of the entire microgrid configuration.

2.6 OPTIMISATION ALGORITHM

Optimization is very beneficial and important to many human applications in many areas. Optimization can be defined as the maximization of output with quality and minimization of input resources. Optimization has applications in many fields like science, technology, economics, and engineering (Babalola et al., 2020). The heuristic algorithm can explore the approximate solution to a problem and the successful result is not always guaranteed. The heuristic algorithm candidates are measured by performance metrics such as lower running time and quality of results (Rashid & Tao, 2018).

A metaheuristic is a type of stochastic-based optimization. Metaheuristic algorithms usually take the idea from how nature is working like GA, Ant Colony Optimization (ACO), and PSO. Metaheuristics algorithms also can be classified based on the mechanisms which are mutation and adaptive (Wong & Ming, 2019). Table 2.3 shows metaheuristic algorithms classification.

Table 2.3: Metaheuristic Algorithms Classification (Wong & Ming, 2019)

Categories	Examples
Swarm intelligence	ACO
Pheromone	Intelligent Water Drop Gravitational search algorithm Glowworm algorithm PSO
Evolutionary	Imperialist Algorithm SaDe L-Shade Differential algorithm GA
Other nature inspiration	Bat algorithm Artificial Bee Colony Optimization Artificial Immune Algorithm Ying Yang Algorithm CSA

2.6.1 Genetic Algorithm

GA was established by John Holland from the University of Michigan in the 1960s, but the popularity of GA come after the 1990s. The mechanism of this algorithm is inspired by the Darwinian Theory of Natural Selection. The steps of GA involve mutations, crossover, and selection. The first step in GA is the generation of a random initial population. Each contains a set of features called chromosomes was being mutated and crossover with other

individuals. This process was iterated many times (Immanuel & Chakraborty, 2019). Figure 2.6 shows a general GA pseudocode and Figure 2.7 shows a flowchart of GA.

```
1 Start
2 Initialize population randomly (say P)
3 Define fitness function of the problem
4 Determine the fitness of the population
5 while !Converging or Optimum not achieved do
6   | Parent selection from population
7   | Crossover operation for new population generation
8   | Perform mutation on the new population
9   | Calculate fitness of new population
10 end
11 If optimum achieved, display the final result
12 Stop
```

Figure 2.6: General GA pseudocode (Immanuel & Chakraborty, 2019)

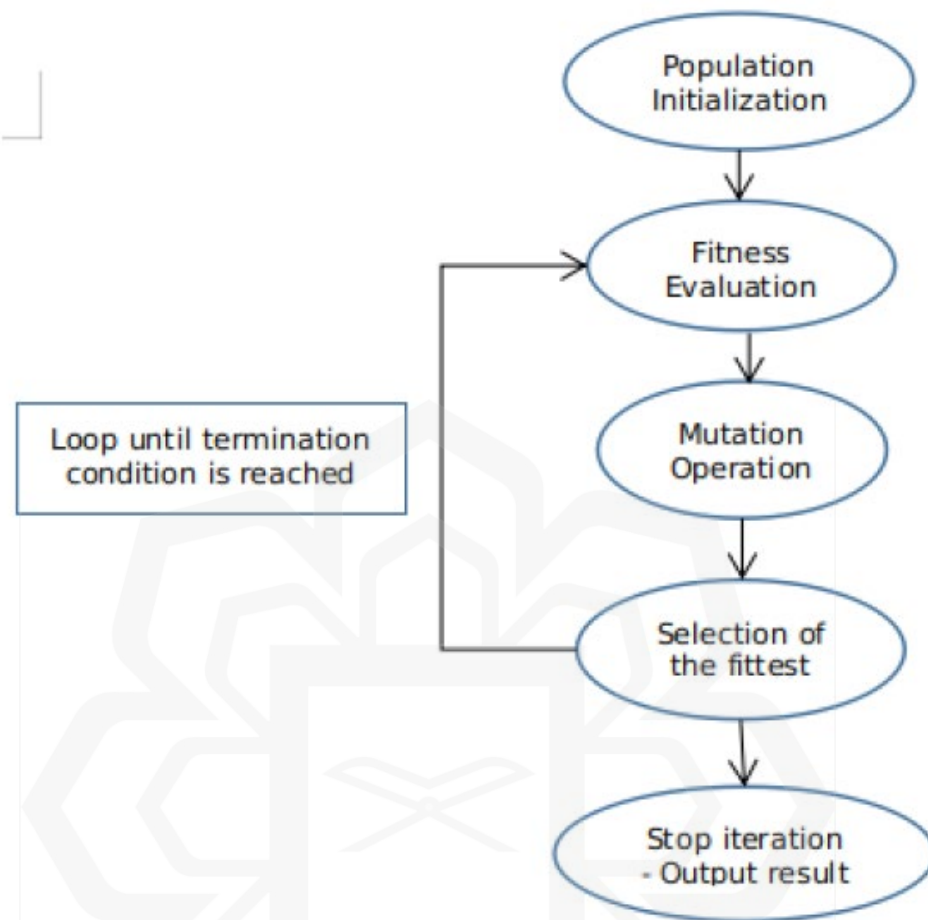


Figure 2.7: GA Flow Chart (Immanuel & Chakraborty, 2019)

2.6.2 Particle Swarm Optimisation

PSO was designed by Kennedy and Eberhart to imitate and simulate simplified social behavior. PSO also can optimize nonlinear problems by the inspiration from fish schooling, bird flocking, and swarming theory in general (Kennedy & Eberhart, 2010). Besides that, PSO has excellent good convergence in addition to best in nonlinear problem optimization. Because of this advantage, many researchers are increasing PSO performance by

introducing new methods and adding new parameters. For example, Eberhart and Shi were introducing linear decreasing weight PSO which decreases the inertia of individual particles by updating them into velocity (Xiaoqing et al., 2019).

The concept of PSO is every individual was following their leader, in this case, Global Best (*gbest*), and track their position simultaneously. The position of every individual is denoted as Particle Best (*pbest*). PSO also has a few parameters such as cognitive parameters, c_1 , social parameters, c_2 , inertia, w and velocity, v_i (Ülker & Ülker, 2018). Figure 2.8 shows the general steps of PSO.

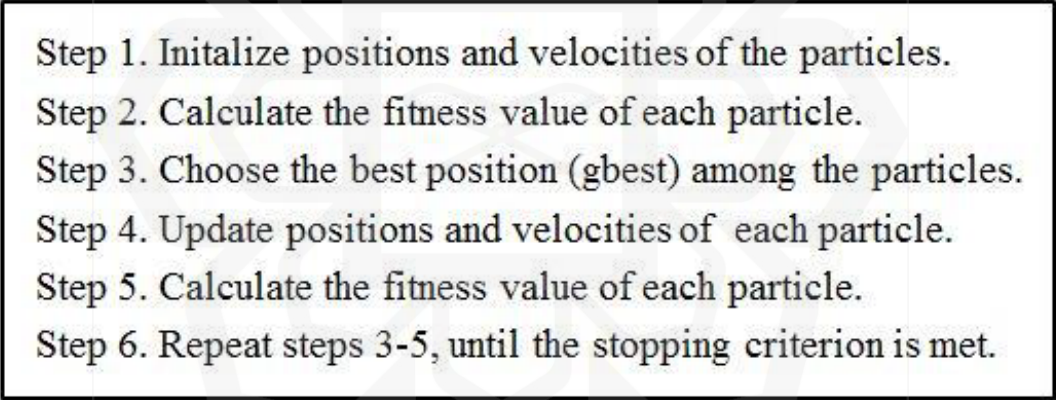
- 
- Step 1. Initialize positions and velocities of the particles.
 - Step 2. Calculate the fitness value of each particle.
 - Step 3. Choose the best position (*gbest*) among the particles.
 - Step 4. Update positions and velocities of each particle.
 - Step 5. Calculate the fitness value of each particle.
 - Step 6. Repeat steps 3-5, until the stopping criterion is met.

Figure 2.8: General steps of PSO (Ülker & Ülker, 2018)

2.6.3 Cuckoo Search Algorithm

CSA was inspired by the behavior of certain cuckoo species. As a part of their reproduction strategy, cuckoo engages in a parasitic way to ensure their offspring hatch and live. Species

like *Guira* and *ani* place their eggs in a shared nest and sometimes eliminate others' eggs to improve their own egg's survival probability. Some species of cuckoo birds lay their eggs in other host birds' nests, and it can be another species of bird. A host bird was throwing another bird's egg or abandon the nest if it found that there are other bird's eggs in the nest. The survival of cuckoo offspring is better in the nest as cuckoo lay their eggs in the nest which is the host bird are just laying the egg. Thus, cuckoo bird offspring was removing other eggs in the nest to increase the food given to them by the host bird (Yang & Deb, 2009).

Besides that, CSA also utilizes Levy Flights which mimic many animals and many insects' patterns to explore their area. The mechanism is a sudden 90-degree turn in their exploration after many straight flight paths. Human behavior also can be related to Levy flight, such as hunter-gatherer foraging. Moreover, light also shows Levy's flight pattern (Yang & Deb, 2009). Figure 2.9 shows the pseudocode of CSA via Levy Flight and Figure 2.10 shows Levy Flight path simulation in a 2-D plane.

Cuckoo Search via Lévy Flights

```
begin  
  Objective function  $f(\mathbf{x})$ ,  $\mathbf{x} = (x_1, \dots, x_d)^T$   
  Generate initial population of  
     $n$  host nests  $\mathbf{x}_i$  ( $i = 1, 2, \dots, n$ )  
  while ( $t < \text{MaxGeneration}$ ) or (stop criterion)  
    Get a cuckoo randomly by Lévy flights  
    evaluate its quality/fitness  $F_i$   
    Choose a nest among  $n$  (say,  $j$ ) randomly  
    if ( $F_i > F_j$ ),  
      replace  $j$  by the new solution;  
    end  
    A fraction ( $p_a$ ) of worse nests  
      are abandoned and new ones are built;  
    Keep the best solutions  
      (or nests with quality solutions);  
    Rank the solutions and find the current best  
  end while  
  Postprocess results and visualization  
end
```

Figure 2.9: Pseudocode of CSA via Levy Flights (Yang & Deb, 2009)

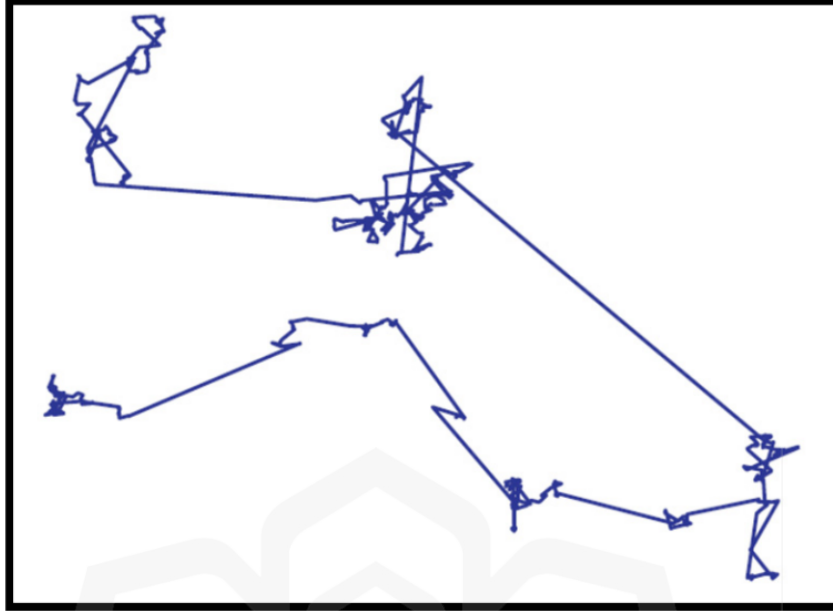


Figure 2.10: Levy Flight Path simulation in 2-D Plane (Ali et al., 2021)

The steps of CSA works are: 1) Cuckoo bird lay their one egg only at one time and put it in a random nest; 2) The best nest which is the higher quality survives for the next generation; 3) The host nest number is always fixed but the cuckoo bird's egg can be detected by host bird with a probability between 0 to 1, denoted as p_a . If that happened, the host bird either abandons the nest or throws discovered egg (Yang & Deb, 2009).

In the findings by Yang et al., CSA performed better than PSO and GA (Yang & Deb, 2009), In comparison with GA, CSA can find global optima 100% in all functions meanwhile GA can find between 77% to 100% of the time to find global optima as shown in Table 2.4. Besides that, PSO can only find between 90% to 100% of the time to find global optima as shown in Table 2.5.

Table 2.4: Comparison of GA and CSA (Yang & Deb, 2009)

Functions/Algorithms	GA	CS
Multiple peaks	52124 ± 3277 (98%)	927 ± 105 (100%)
Michalewicz's ($d=16$)	89325 ± 7914 (95%)	3221 ± 519 (100%)
Rosenbrock's ($d=16$)	55723 ± 8901 (90%)	5923 ± 1937 (100%)
De Jong's ($d=256$)	25412 ± 1237 (100%)	4971 ± 754 (100%)
Schwefel's ($d=128$)	227329 ± 7572 (95%)	8829 ± 652 (100%)
Ackley's ($d=128$)	32720 ± 3327 (90%)	4936 ± 903 (100%)
Rastrigin's	110523 ± 5199 (77%)	10354 ± 3755 (100%)
Easom's	19239 ± 3307 (92%)	6751 ± 1902 (100%)
Griewanks	70925 ± 7652 (90%)	10912 ± 4050 (100%)
Shubert's (18 minima)	54077 ± 4997 (89%)	9770 ± 3592 (100%)

Table 2.5: Comparison of PSO and CS (Yang & Deb, 2009)

Functions/Algorithms	GA	CS
Multiple peaks	3719 ± 205 (97%)	927 ± 105 (100%)
Michalewicz's ($d=16$)	6922 ± 537 (98%)	3221 ± 519 (100%)
Rosenbrock's ($d=16$)	32756 ± 5325 (98%)	5923 ± 1937 (100%)
De Jong's ($d=256$)	17040 ± 1123 (100%)	4971 ± 754 (100%)
Schwefel's ($d=128$)	14522 ± 1275 (97%)	8829 ± 652 (100%)
Ackley's ($d=128$)	23407 ± 4325 (92%)	4936 ± 903 (100%)
Rastrigin's	79491 ± 3715 (90%)	10354 ± 3755 (100%)
Easom's	17273 ± 2929 (90%)	6751 ± 1902 (100%)

Griewanks	55970 ± 4223 (92%)	10912 ± 4050 (100%)
Shubert's (18 minima)	23992 ± 3755 (92%)	9770 ± 3592 (100%)

Uniyal et. al. find total DG sizing and location are nearly equal, meanwhile, real power loss is even less (Uniyal & Kumar, 2016), The highest power loss reduction in the study is CSA and PSO at the same par. While Gravitational Search Algorithm (GSA) is the third place, and the worst is GA.

An algorithm is needed to explore an optimum configuration of a microgrid. CSA is used in this research to find the optimum network reconfiguration topology. Compared to PSO, CSA is more effective and consist of fewer parameter, thus making the implementation easier compared to PSO. Thus, in this research, power loss minimization and voltage stability were conducted by using CSA as the algorithm to find the solution for the power flow metaheuristic problem. The simulation results were compared with GA and PSO.

2.7 RELATED WORKS

Table 2.6 shows the related works about techniques used to reconfigure the network with EV charging loads integration. All research shows a reduction in power loss when a network is reconfigured by an optimization algorithm. Among these research, Li et al. (2015) and J. Wang et al. (2022) used a convex optimization algorithm whereas other researchers used a metaheuristics optimization algorithm.

Table 2.6: Table of Related Works

Authors (Year)	Approach	Contribution	Limitation
Li et al. (2015)	Distribution Network Reconfiguration based on Second-order Conic Programming Considering EV Charging Strategy	Distribution Network Reconfiguration with EV charging load penetration using Second-order Conic Programming has lower power loss compared to PSO	Consumed time to calculate power loss is higher by using Second-order Conic Programming compared to PSO
Reddy et al. (2021)	Minimization of EV charging Stations influence on unbalanced radial distribution system with optimal reconfiguration using PSO	Power loss can be reduced on an unbalanced radial distribution system by using PSO up to 26.36%.	The simulation was conducted on an unbalanced IEEE-19 bus system which is a small-scale distribution system.
Wan Izzat Aiman et al. (2021)	CSA is used to find optimal reconfiguration with EV charging load integrated	CSA can discover the optimum configuration to minimize power loss	Only power loss reduction is used as an objective function.

<p>Zhechao Li et al. (2016)</p>	<p>Reconfiguration to Enhance the Capacity of EV Charging Stations in Radial Distribution Systems by using PSO</p>	<p>PSO can reduce power loss and at the same time increase EV charging load capacity as the number of EV charging station bus site increase, the power loss reduces from 355.64 kW to 293.67 kW, and EV charging station capacity increases from 4,744 kW to 5,249kW.</p>	<p>Bus 9, 14, 20, and 56 were assumed as potential EV charging stations bus sites without proper explanation.</p>
<p>Reddy & Selvajyothi (2020)</p>	<p>Mitigation of the impact of EV charging stations in the radial distribution system by using PSO by finding optimal placement of EV charging stations and network reconfiguration</p>	<p>PSO can minimize power loss and voltage profile better when reconfiguration is run simultaneously with EV charging station placement compared to EV charging station placement only.</p>	<p>The simulation was run on a balanced radial distribution system. The study can be extended to the unbalanced radial distribution system.</p>
<p>J. Wang et al. (2022)</p>	<p>Coordinated distribution reconfiguration with maintenance scheduling considering EV charging uncertainty</p>	<p>Second-Order Cone Relaxation can find solutions to reduce power loss considering EV charging uncertainty when the distribution</p>	<p>There is no comparison with metaheuristics optimization algorithms like CSA and PSO</p>

	by using Second-Order Cone Relaxation	reconfiguration system is under maintenance	
--	---------------------------------------	---	--

2.8 SUMMARY

In summary, an algorithm is needed to find the optimum power loss minimization and voltage stability in the case of microgrid reconfiguration. CSA is chosen as the algorithm in this research with the simulation was compared with PSO and GA as CSA may perform better to find the optimal solution when power loss minimization and voltage stability is the objective function.

Thus, in this study, EV charging load was integrated with the IEEE-33 bus system and IEEE-69 bus system as the simulations to find optimal power loss and voltage stability. EV charging load has a big influence on microgrid power loss and voltage stability especially when fast charging is integrated. Reconfiguration of the microgrid can be used as a method to reduce power loss and increase voltage stability. CSA is used to discover the optimal reconfiguration in respect of power loss minimization and voltage stability. The findings between CSA, PSO, and GA were compared and analyzed.

CHAPTER THREE

RESEARCH METHODOLOGY

3.1 OVERVIEW

In this research, the microgrid power flow was being evaluated by using the MATLAB program. The approximation technique to find bus voltage magnitude and voltage angle is by using the Newton-Raphson (N-R) technique. Meanwhile, the microgrid model is based on the IEEE-33 bus system and IEEE-69 bus system. IEEE-33 bus system line and bus data are based on Baran & Wu (1989) and IEEE-69 bus system line and the bus is based on Chiang & Jean-Jumeau (1990). The IEEE-33 bus system is the simulation of a small-scale microgrid and the IEEE-69 bus system is the simulation of a medium-scale microgrid.

Then, the objective of this research is to find the best solution for network reconfiguration with EV charging load integrated by finding the optimum voltage stability and power loss as a single objective.

3.2 POWER FLOW

3.2.1 Power Flow Formulation

Power flow, also known as load flow, is generally used to operate and plan a power system. Power flow is calculated from generation, load, and network data. The output of the

calculation is power loss, line flow, and voltages of every bus. As these equations are nonlinear, the power flow problem was calculated by using iterative methods. The output can be solved by calculating power balance equations (Albadi, 2020). In this research, the technique used is the N-R technique.

The power flow objective is to calculate the voltage of each bus which is the magnitude and angle by using data of generation, load, and network condition. Line flows and power losses can be calculated as the voltage is known. To solve the power flow problem, known and unknown variables are needed to be identified, and based on this identification, buses are categorized as a generation, slack, and load buses. A slack bus is considered a reference bus as both magnitude and angle was provided in the system; thus, it is also called a swing bus. Other generators are called PV buses as real power is specified but the angle is unknown. Meanwhile, load buses are known as PQ buses because real and reactive power loads are determined. But in PQ buses, voltage magnitude and voltage angles are unspecified, meanwhile, in PV buses, only the voltage angle is unidentified (Albadi, 2020). In this research, only the slack bus and PQ bus are used in the distribution system power flow analysis. The slack bus is bus number 1 in all bus system simulations and the other buses are PQ buses. So, there is only one generation node in the distribution system which is the slack bus. Table 3.1 shows bus type in the power flow problem.

Table 3.1: Bus type in power flow problem (Albadi, 2020)

Bus Type	Voltage ($ V_i \angle \delta_i$)		Real Power			Reactive Power		
	Magnitude	Angle	Generation	Load	Net (P_i)	Generation	Load	Net (Q_i)
Slack/Swing	Specified	Specified	Unknown	Specified	Unknown	Unknown	Specified	Unknown
Generator/Regulated/PV	Specified	Unknown	Specified	Specified	Specified	Unknown	Specified	Unknown
Load/PQ	Unknown	Unknown	Specified	Specified	Specified	Specified	Specified	Specified

3.2.2 Power Flow Equation and Admittance Matrix

Power flow formulation can be modeled in an abstract mathematical model which is the admittance matrix. It is also known as the Y-bus matrix. The matrix consists of lines and bus values. The matrix is a square matrix with the bus number taken as its dimensions.

$$Y = \begin{bmatrix} Y_{11} & \cdots & Y_{1n} \\ \vdots & \ddots & \vdots \\ Y_{n1} & \cdots & Y_{nn} \end{bmatrix} \quad (1)$$

whereas, n is the number of buses.

Value of Y_{ii} is equal to summation of admittance connected to Y_i . Meanwhile, elements Y_{ij} are the negative values of the admittance between buses i and j . In a large system, Y -bus is a sparse matrix.

$$Y_{11} = \sum_{\substack{j=0 \\ j \neq i}}^n y_{ij} \quad (2)$$

$$Y_{ij} = Y_{ji} = -y_{ij} \quad (3)$$

Net injected power of any bus can be solved by using bus voltage V_i , neighbor voltage V_j , and admittance between the bus and neighboring bus, y_{ij} . Figure 3.1 shows the flow of current to the load bus.

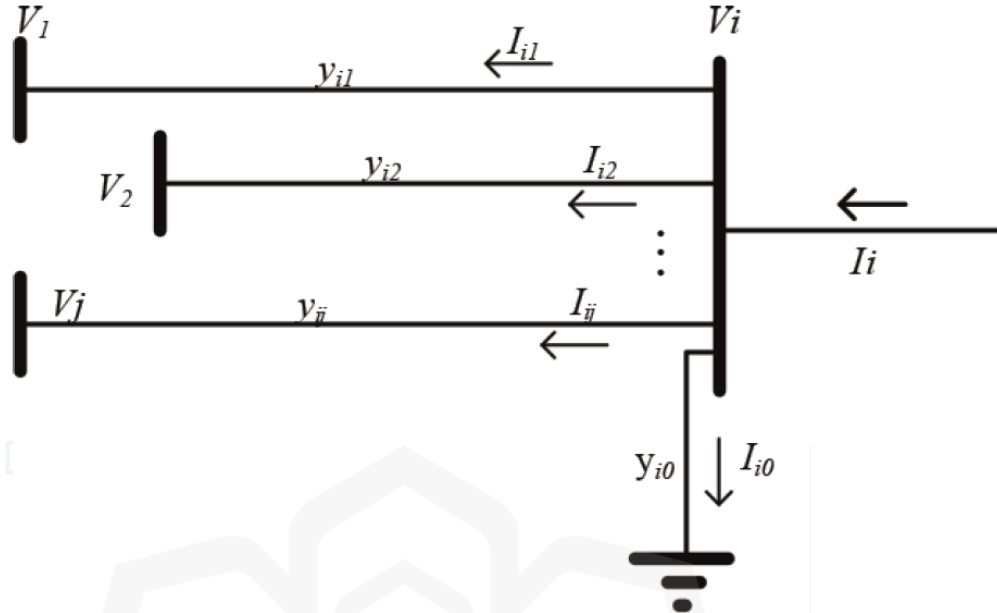


Figure 3.1: Flow of current to load bus (Albadi, 2020)

$$I_i = V_i y_{i0} + (V_i - V_1) y_{i1} + (V_i - V_2) y_{i2} + \dots + (V_i - V_j) y_{ij} \quad (4)$$

Rearrange the equation as voltage function:

$$I_i = V_i (y_{i0} + y_{i1} + y_{i2} + \dots + y_{ij}) - V_1 y_{i1} - V_2 y_{i2} - \dots - V_j y_{ij} \quad (5)$$

$$I_i = V_i \sum_{\substack{j=0 \\ j \neq i}} y_{ij} - \sum_{\substack{j=1 \\ j \neq i}} y_{ij} V_j = V_i Y_{ii} + \sum_{\substack{j=1 \\ j \neq i}} Y_{ij} V_j \quad (6)$$

The power equation of any bus is:

$$S_i = P_i + jQ_i = P_i I_i^* \quad (7)$$

Which also can be expressed as:

$$S_i^* = P_i - jQ_i = V_i^* I_i \quad (8)$$

By substituting I_i into power equation:

$$S_i^* = V_i^* \left(V_i \sum_{\substack{j=0 \\ j \neq i}} y_{ij} - \sum_{\substack{j=1 \\ j \neq i}} y_{ij} V_j \right) = V_i^* \left(V_i Y_{ii} + \sum_{\substack{j=1 \\ j \neq i}} Y_{ij} V_j \right) \quad (9)$$

Real and reactive power can be calculated by:

$$P_i = Re \left\{ V_i^* \left(V_i \sum_{\substack{j=0 \\ j \neq i}} y_{ij} - \sum_{\substack{j=1 \\ j \neq i}} y_{ij} V_j \right) \right\} = Re \left\{ V_i^* \left(V_i Y_{ii} + \sum_{\substack{j=1 \\ j \neq i}} Y_{ij} V_j \right) \right\} \quad (10)$$

$$Q_i = -Im \left\{ V_i^* \left(V_i \sum_{\substack{j=0 \\ j \neq i}} y_{ij} - \sum_{\substack{j=1 \\ j \neq i}} y_{ij} V_j \right) \right\} = -Im \left\{ V_i^* \left(V_i Y_{ii} + \sum_{\substack{j=1 \\ j \neq i}} Y_{ij} V_j \right) \right\} \quad (11)$$

Also, can be expressed as:

$$P_i = \sum_{j=1}^n |V_i||V_j||Y_{ij}| \cos(\theta_{ij} - \delta_i + \delta_j) \quad (12)$$

$$Q_i = - \sum_{j=1}^n |V_i||V_j||Y_{ij}| \sin(\theta_{ij} - \delta_i + \delta_j) \quad (13)$$

Thus, I_i can be expressed as:

$$I_i = \frac{P_i - jQ_i}{V_i^*} = V_i \sum_{\substack{j=0 \\ j \neq i}} y_{ij} - \sum_{\substack{j=1 \\ j \neq i}} y_{ij} V_j = V_i Y_{ii} + \sum_{\substack{j=1 \\ j \neq i}} Y_{ij} V_j \quad (14)$$

3.2.3 Newton-Raphson Technique

The N-R technique is a technique based on Taylor's expansion approximation, which is also known as the method of successive approximation. The objective of the N-R technique is to find variable x when the function is $f(x) = c$. This function can be calculated by Taylor's expansion approximation.

To find variable x , we need to start with an initial estimate of $x^{[0]}$ and a deviation from the correct solution of $\Delta x^{[0]}$. Thus, the function is:

$$f(x^{[0]} + \Delta x^{[0]}) = c \quad (15)$$

By utilizing Taylor's expansion into c , the equation can be expressed as:

$$= f(x^{[0]}) + f'(x^{[0]})\Delta x^{[0]} + \frac{1}{2!}f''(x^{[0]})\Delta x^{[0]2} + \frac{1}{3!}f'''(x^{[0]})\Delta x^{[0]3} + \dots = c \quad (16)$$

As $\Delta x^{[0]}$ is too small, the higher order term $(+ \frac{1}{2!}f''(x^{[0]})\Delta x^{[0]2} + \frac{1}{3!}f'''(x^{[0]})\Delta x^{[0]3} + \dots)$ can be neglected and approximation can be calculated by using the first two terms.

$$f(x^{[0]} + \Delta x^{[0]}) \approx f(x^{[0]}) + f'(x^{[0]})\Delta x^{[0]} = c \quad (17)$$

Deviation from the right solution can be calculated iteratively from $x^{[0]}$ as the following equation:

$$x^{[0]} = \frac{c - f(x^{[0]})}{f'(x^{[0]})} = \frac{\Delta f(x^{[0]})}{f'(x^{[0]})} \quad (18)$$

Thus, the next iteration, which is $x^{[1]}$ improve as follows:

$$x^{[1]} = x^{[0]} + \Delta x^{[0]} \quad (19)$$

The iterative process is terminated if differences between calculated and scheduled value $(\Delta f^{[k]} = c - f(x^{[k]}))$ is not exceeded the acceptable limit $|\Delta f^{[k]}| \leq \varepsilon$.

In the power flow problem aspect, variable x is voltage magnitude and angle ($|V_i| \angle \delta_i$) at load buses. The variable c is both load bus net real, P_i^{sch} and reactive power, jQ_i^{sch} .

Thus, the load bus net real power iterative value is:

$$P_i^{k+1} = \sum_{j=1}^n |V_i|^k |V_j|^{k \text{ or } k+1} |Y_{ij}| \cos(\theta_{ij} - \delta_i^{[k]} + \delta_j^{[k]}) \quad (20)$$

As many variables are being calculated, the Jacobian matrix can be used as partial derivatives is being used in respect to many variables. The Jacobian matrix can be expressed as follow:

$$f' = \begin{bmatrix} \frac{\partial P_i}{\partial \delta_i} & \frac{\partial P_i}{\partial |V_i|} \\ \frac{\partial Q_i}{\partial \delta_i} & \frac{\partial Q_i}{\partial |V_i|} \end{bmatrix} = \begin{bmatrix} J_{P\delta} & J_{P|V|} \\ J_{Q\delta} & J_{Q|V|} \end{bmatrix} \quad (21)$$

Thus, the N-R method can solve the power flow problem by using the following equation:

$$\begin{bmatrix} P_i^{sch} \\ Q_i^{sch} \end{bmatrix} - \begin{bmatrix} P_i^{[k]} \\ Q_i^{[k]} \end{bmatrix} = \begin{bmatrix} \Delta P_i^{[k]} \\ \Delta Q_i^{[k]} \end{bmatrix} = \begin{bmatrix} \frac{\partial P_i^{[k]}}{\partial \delta_i} & \frac{\partial P_i^{[k]}}{\partial |V_i|} \\ \frac{\partial Q_i^{[k]}}{\partial \delta_i} & \frac{\partial Q_i^{[k]}}{\partial |V_i|} \end{bmatrix} \begin{bmatrix} \Delta \delta_i^{[k]} \\ \Delta |V_i|^{[k]} \end{bmatrix} \quad (22)$$

An inverse Jacobian matrix is needed to calculate deviation for all iterations:

$$\begin{bmatrix} \Delta \delta_i^{[k]} \\ \Delta |V_i|^{[k]} \end{bmatrix} = \begin{bmatrix} J_{P\delta}^{[k]} & J_{P|V|}^{[k]} \\ J_{Q\delta}^{[k]} & J_{Q|V|}^{[k]} \end{bmatrix}^{-1} \begin{bmatrix} \Delta P_i^{[k]} \\ \Delta Q_i^{[k]} \end{bmatrix} \quad (23)$$

After that, the new iteration can be solved by:

$$\begin{bmatrix} \delta_i^{[k]} \\ |V_i|^{[k]} \end{bmatrix} = \begin{bmatrix} \delta_i^{[k-1]} \\ |V_i|^{[k-1]} \end{bmatrix} + \begin{bmatrix} \Delta \delta_i^{[k]} \\ \Delta |V_i|^{[k]} \end{bmatrix} \quad (24)$$

The operation is continued until the differences between scheduled and calculated values are within the acceptable range, $\begin{bmatrix} \Delta P_i^{[k]} \\ \Delta Q_i^{[k]} \end{bmatrix} \leq \varepsilon$.

In this research, the number of iteration processes using the N-R technique is 10 iterations for the IEEE-33 bus system and IEEE-69 bus system for all algorithms used in this research. If the solution is not found within 10 iterations, the calculation is considered as do not converge. Meanwhile, the acceptable range of ε is within 10^{-8} .

3.3 IEEE BUS SYSTEM

3.3.1 IEEE-33 Bus System

IEEE-33 bus system have 33 buses, which is 32 buses is load bus and 1 bus is the generator bus. In terms of switches, IEEE-33 consists of 37 switches, which are 32 sectionalizing switches and five tie switches. The base voltage of IEEE-33 buses system is 12.66 kV. The total real power load is 3.72 MW, and the total reactive power is 2.30 MVAR. The initial tie switch reconfiguration is 33, 34, 35, 36, and 37. The data for all buses and switches are shown in table below. Real power and reactive power in data table is the load connected to 'to bus'. IEEE-33 bus system is a power distribution system data for a simulation in a small scale microgrid. Table 3.2 shows data of IEEE-33 bus system used in this research.

Table 3.2: Data of IEEE-33 bus system

Line No	From Bus	To Bus	R (Ω)	X (Ω)	Real Power (kW)	Reactive Power (kVAR)
1	1	2	0.0922	0.0470	100	60
2	2	3	0.4930	0.2511	90	40
3	3	4	0.3660	0.1864	120	80
4	4	5	0.3811	0.1941	60	30
5	5	6	0.8190	0.7070	60	20
6	6	7	0.1872	0.6188	200	100
7	7	8	0.7114	0.2351	200	100
8	8	9	1.0300	0.7400	60	20
9	9	10	1.0440	0.7400	60	20
10	10	11	0.1966	0.0650	45	30
11	11	12	0.3744	0.1238	60	35
12	12	13	1.4680	1.1550	60	35
13	13	14	0.5416	0.7129	120	80
14	14	15	0.5910	0.5260	60	10
15	15	16	0.7463	0.5450	60	20
16	16	17	1.2890	1.7210	60	20
17	17	18	0.7320	0.5740	90	40
18	2	19	0.1640	0.1565	90	40
19	19	20	1.5042	1.3554	90	40
20	20	21	0.4095	0.4784	90	40
21	21	22	0.7089	0.9373	90	40
22	3	23	0.4512	0.3083	90	50
23	23	24	0.8980	0.7091	420	200
24	24	25	0.8960	0.7011	420	200
25	6	26	0.2030	0.1034	60	25

26	26	27	0.2842	0.1447	60	25
27	27	28	1.0590	0.9337	60	20
28	28	29	0.8042	0.7006	120	70
29	29	30	0.5075	0.2585	200	600
30	30	31	0.9744	0.9630	150	70
31	31	32	0.3105	0.3619	210	100
32	32	33	0.3410	0.5302	60	40
33	21	8	2.0000	2.0000	-	-
34	9	15	2.0000	2.0000	-	-
35	12	22	2.0000	2.0000	-	-
36	18	33	0.5000	0.5000	-	-
37	25	29	0.5000	0.5000	-	-

In the IEEE-33 bus system, there are 5 fundamental loops in the microgrid bus system. At one time, only one tie switch in a fundamental loop is needed to be open. Thus, at one time, five switches were being opened, one switch by each fundamental loop. By using this method, all busloads were confirmed to be interconnected with the generator bus. Table 3.3 shows fundamental loop of IEEE-33 used in this research.

Table 3.3: Fundamental Loop of IEEE-33 bus system

Fundamental Loop Number	Tie-Line
1	2, 3, 4, 5, 6, 7, 18, 19, 20, 33
2	9, 10, 11, 12, 13, 14, 34

3	2, 3, 4, 5, 6, 7, 8, 9, 10, 11, 18, 19, 20, 21, 35
4	6, 7, 8, 9, 10, 11, 12, 13, 14, 15, 16, 17, 25, 26, 27, 28, 29, 30, 31, 32, 36
5	3, 4, 5, 22, 23, 24, 25, 26, 27, 28, 37

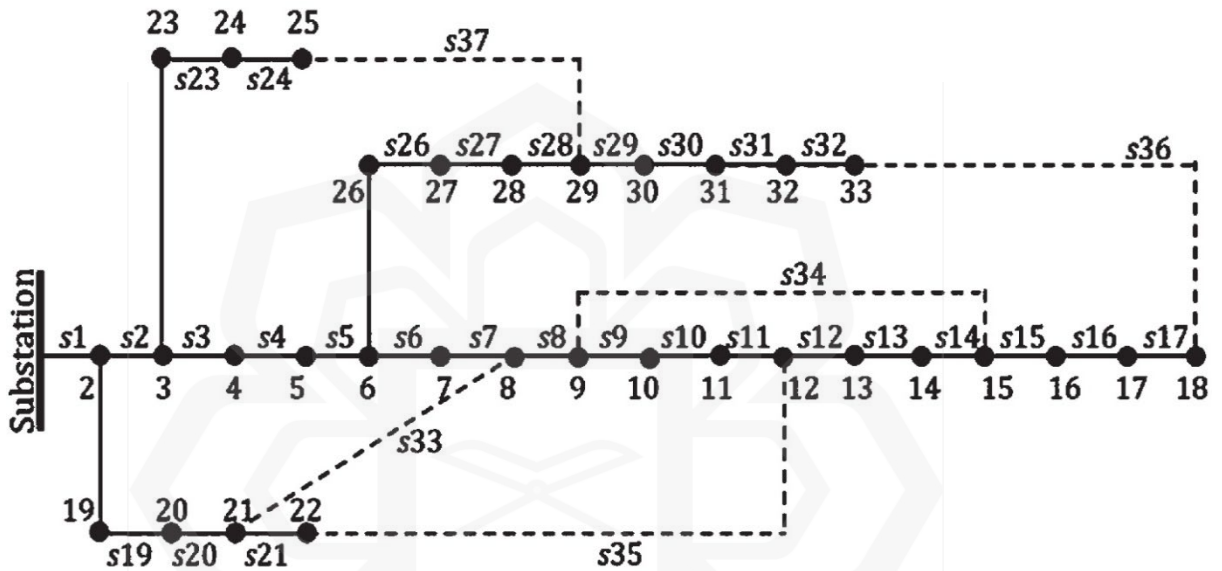


Figure 3.2: IEEE-33 initial configuration

There are seven index cases that was being simulated in the IEEE-33 bus system. The initial configuration of IEEE-33 for tie and sectionalize switch in all indexes is shown in Figure 3.2. Index 0 is a simulation when there is no EV charging station load integrated into the microgrid system. Index 1 is a simulation of one fast-charging station with a load of 1500 kW connected to bus 2, which is the strongest bus. A strong bus in this IEEE-33 bus system means the bus is more unlikely to collapse in case of additional load is added to the system compared to other buses as the bus has the highest VSI compared to other

buses. 1500kW charging load is equivalent to 30 EVs to charge at the same time in one station by using a 50kW fast charger.

Index 2 is the simulation of two charging stations connected to bus 2, which is a 3000kW load, which can cater to up to 60 EVs at the same time. Index 3 is the simulation of five charging stations connected to bus 2, which is a 7500kW load, thus, this simulation simulates 150 EVs using the charging station at the same time. Index 4 is a simulation of two charging stations connecting to the microgrid system, one connected to bus 2 and the other connected to bus 19. Bus 19 is the second strongest bus. Thus, a 3000kW load is connected to the system. Index 5 is a 1500kW load connected to bus 18. Bus 18 is the weakest bus in the microgrid system. Meanwhile, index 6 is 1500kW each are connected to bus 18 and bus 17, thus the load connected to the system is 3000kW. Bus 17 is the second weakest bus in the system. For example, Figure 3.3 is the illustration of index 1 which is one EV charging station load connected to bus 2. Table 3.4 shows index cases of IEEE-33 bus system.

Table 3.4: Index cases of IEEE-33 bus system (Deb, Tammi, et al., 2018)

Index	Details	EV charging load (kW)
0	No EV charging load	0
1	Fast charging load at bus 2	1500
2	Fast charging load at bus 2	3000
3	Fast charging load at bus 2	7500
4	Fast charging load at bus 2 and bus 19	3000 (1500 each bus)
5	Fast charging load at bus 18	1500
6	Fast charging load at bus 18 and bus 17	3000 (1500 each bus)

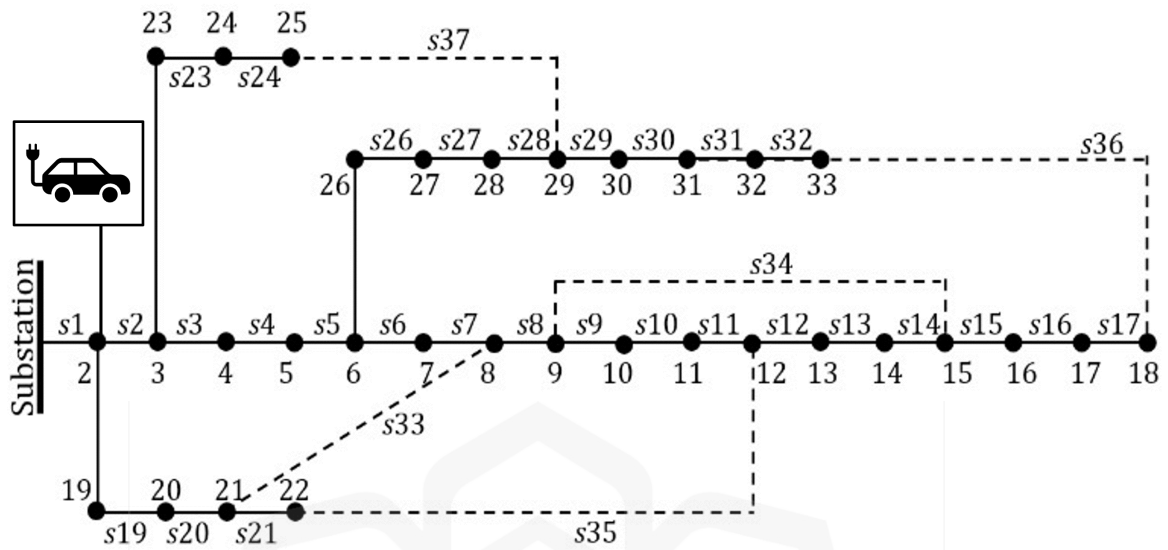


Figure 3.3: Index 1 of IEEE-33 bus system (1500 kW at bus 2)

3.3.2 IEEE-69 Bus System

IEEE-69 bus system consists of 69 buses, which is 68 buses is load bus and 1 bus is the generator bus. In terms of switches, IEEE-69 consists of 73 switches, which are 68 sectionalizing switches and five tie switches. The base voltage of IEEE-69 buses system is 12.66 kV. The total real power load is 3.80 MW, and the total reactive power is 2.69 MVAR. The initial tie switch reconfiguration is 69, 70, 71, 72, and 73. The data for all buses and switches are shown in the table below. Real power and reactive power in the data table is the load connected to 'to bus'. The IEEE-69 bus system is a power system data for a simulation in a medium-scale microgrid system. There are also five fundamental loops in the IEEE-69 bus system. Figure 3.4 shows IEEE-69 initial reconfiguration and Table 3.5 shows data of IEEE-69 used in the research.

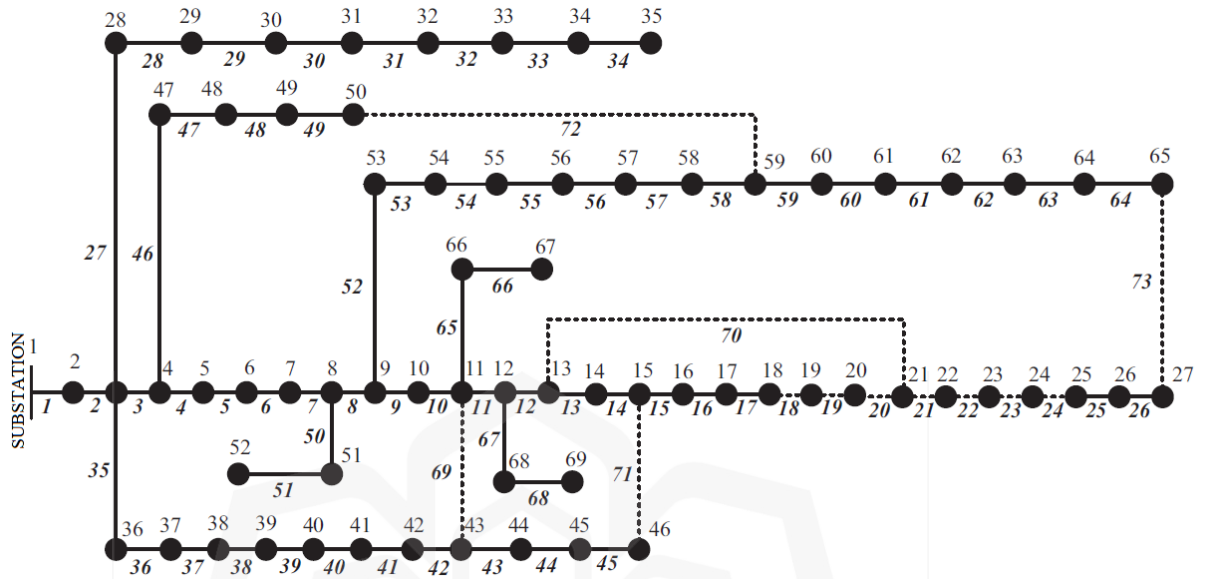


Figure 3.4: IEEE-69 initial reconfiguration (Nguyen et al., 2016)

Table 3.5: Data of IEEE-69 bus system

Line No	From Bus	To Bus	R (Ω)	X (Ω)	Real Power (kW)	Reactive Power (kVAR)
1	1	2	0.0005	0.0012	0	0
2	2	3	0.0005	0.0012	0	0
3	3	4	0.0015	0.0036	0	0
4	4	5	0.0251	0.0294	0	0
5	5	6	0.3660	0.1864	2.6	2.2
6	6	7	0.3811	0.1941	40.4	30
7	7	8	0.0922	0.0470	75	54
8	8	9	0.0493	0.0251	30	22

9	9	10	0.8190	0.2707	28	19
10	10	11	0.1872	0.0619	145	104
11	11	12	0.7114	0.2351	145	104
12	12	13	1.0300	0.3400	8	5.5
13	13	14	1.0440	0.3450	8	5.5
14	14	15	1.0580	0.3496	0	0
15	15	16	0.1966	0.0650	45.5	30
16	16	17	0.3744	0.1238	60	35
17	17	18	0.0047	0.0016	60	35
18	18	19	0.3276	0.1083	0	0
19	19	20	0.2106	0.0696	1	0.6
20	20	21	0.3416	0.1129	114	81
21	21	22	0.0140	0.0046	5	3.5
22	22	23	0.1591	0.0526	0	0
23	23	24	0.3463	0.1145	28	20
24	24	25	0.7488	0.2475	0	0
25	25	26	0.3089	0.1021	14	10
26	26	27	0.1732	0.0572	14	10
27	3	28	0.0044	0.0108	26	18.6
28	28	29	0.0640	0.1565	26	18.6
29	29	30	0.3978	0.1315	0	0
30	30	31	0.0702	0.0232	0	0
31	31	32	0.3510	0.1160	0	0
32	32	33	0.8390	0.2816	14	10
33	33	34	1.7080	0.5646	19.5	14
34	34	35	1.4740	0.4873	6	4
35	3	36	0.0044	0.0108	26	18.55
36	36	37	0.0640	0.1565	26	18.55
37	37	38	0.1053	0.1230	0	0

38	38	39	0.0304	0.0355	24	17
39	39	40	0.0018	0.0021	24	17
40	40	41	0.7283	0.8509	1.2	1
41	41	42	0.3100	0.3623	0	0
42	42	43	0.0410	0.0478	6	4.3
43	43	44	0.0092	0.0116	0	0
44	44	45	0.1089	0.1373	39.2	26.3
45	45	46	0.0009	0.0012	39.2	26.3
46	4	47	0.0034	0.0084	0	0
47	47	48	0.0851	0.2083	79	56.4
48	48	49	0.2898	0.7091	384.7	274.5
49	49	50	0.0822	0.2011	384.7	274.5
50	8	51	0.0928	0.0473	40.5	28.3
51	51	52	0.3319	0.1114	3.6	2.7
52	9	53	0.1740	0.0886	4.35	3.5
53	53	54	0.2030	0.1034	26.4	19
54	54	55	0.2842	0.1447	24	17.2
55	55	56	0.2813	0.1433	0	0
56	56	57	1.5900	0.5337	0	0
57	57	58	0.7837	0.2630	0	0
58	58	59	0.3042	0.1006	100	72
59	59	60	0.3861	0.1172	0	0
60	60	61	0.5075	0.2585	1244	888
61	61	62	0.0974	0.0496	32	23
62	62	63	0.1450	0.0738	0	0
63	63	64	0.7105	0.3619	227	162
64	64	65	1.0410	0.5302	59	42
65	11	66	0.2012	0.0611	18	13
66	66	67	0.0047	0.0014	18	13

67	12	68	0.7394	0.2444	28	20
68	68	69	0.0047	0.0016	28	20
69	11	43	0.5000	0.5000	-	-
70	13	21	0.5000	0.5000	-	-
71	15	46	1.0000	1.0000	-	-
72	50	59	2.0000	2.0000	-	-
73	27	65	1.0000	1.0000	-	-

Table 3.6: Fundamental Loop of the IEEE-69 bus system

Fundamental Loop Number	Tie-Line
1	3, 4, 5, 6, 7, 8, 9, 10, 35, 36, 37, 38, 39, 40, 41, 42, 69
2	13, 14, 15, 16, 17, 18, 19, 20, 70
3	3, 4, 5, 6, 7, 8, 9, 10, 11, 12, 13, 14, 35, 36, 37, 38, 39, 40, 41, 42, 43, 44, 45, 71
4	4, 5, 6, 7, 8, 46, 47, 48, 49, 52, 53, 54, 55, 56, 57, 58, 72
5	9, 10, 11, 12, 13, 14, 15, 16, 17, 18, 19, 20, 21, 22, 23, 24, 25, 26, 52, 53, 54, 55, 56, 57, 58, 59, 60, 61, 62, 63, 64, 73

There are seven index cases that were being simulated in the IEEE-69 bus system. Fundamental loops of the IEEE-69 bus system is shown in Table 3.6. Index cases of IEEE-69 is shown in Table 3.7. Index 0 is a simulation when there is no EV charging station load integrated into the microgrid system. Index 1 is a simulation of one fast-charging station with a load of 1500 kW connected to bus 2, which is the strongest bus. A strong bus in this

IEEE-69 bus system means the VSI of the bus is the highest, thus, the bus is more unlikely to collapse in case of additional load is added to the system compared to other buses.

Index 2 is the simulation of two charging stations connected to bus 2, which is a 3000kW load, which can cater to up to 60 EVs at the same time. Index 3 is the simulation of five charging stations connected to bus 2, which is a 7500kW load, thus, this simulation simulates 150 EVs using the charging station at the same time. Index 4 is a simulation of two charging stations connecting to the microgrid system, one connected to bus 2 and the other connected to bus 3. Bus 3 is the second strongest bus. Thus, a 3000kW load is connected to the system. Index 5 is a 1500kW load connected to bus 65. Bus 65 is the weakest bus in the system. Meanwhile, index 6 is 1500kW each are connected to bus 65 and bus 64, thus the load connected to the system is 3000kW. Bus 64 is the second weakest bus in the system. For example, Figure 3.5 is the illustration of index 1 which is one EV charging station load connected to bus 2.

Table 3.7: Index cases of the IEEE-69 bus system

Index	Details	EV charging load (kW)
0	No EV charging load	0
1	Fast charging load at bus 2	1500
2	Fast charging load at bus 2	3000
3	Fast charging load at bus 2	7500
4	Fast charging load at bus 2 and bus 3	3000 (1500 each bus)
5	Fast charging load at bus 65	1500
6	Fast charging load at bus 65 and bus 64	3000 (1500 each bus)

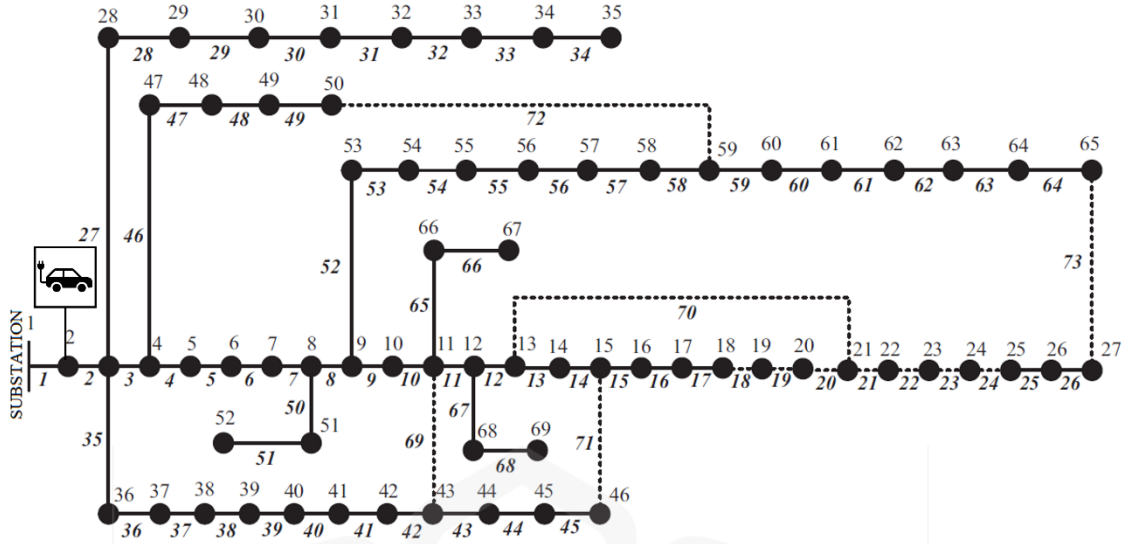


Figure 3.5: Index 1 of IEEE-69 bus system (1500 kW at bus 2)

3.4 OBJECTIVE FUNCTIONS

3.4.1 Power Loss

Total power loss can be evaluated by a power loss summation of all branches in the microgrid system. The equation is given as follows:

$$P_{loss} = \sum_{i=1}^{Nbr} R_i \left(\frac{P_i^2 + Q_i^2}{V_i^2} \right) \quad (25)$$

Then, the net power loss reduction can be calculated as the ratio of power loss after reconfiguration over power loss before reconfiguration. Thus, the value of the net power

loss reduction is less than 1 if there is power loss reduction after reconfiguration. The formulation based on (Nguyen et al., 2016) is given as follow:

$$\Delta P_{loss}^R = \frac{P_{loss}^{rec.}}{P_{loss}^0} \quad (26)$$

3.4.2 Voltage Stability Index

The VSI formulation is taken from research by Ranjan, Venkatesh, & Das (2003), which is given the formula as below:

$$VSI_{(k+1)} = |V_k|^4 - 4(P_{k+1}X_k - Q_{k+1}R_k)^2 - 4(P_{k+1}R_k - Q_{k+1}X_k)|V_k|^2 \quad (27)$$

which is $VSI_{(k+1)}$ being VSI of $k + 1$ node, V_k being voltage of k^{th} node, P_{k+1} being real power loss of $k + 1$ node, X_k being the reactance of k^{th} node, Q_{k+1} being reactive power loss of $k + 1$ node, and R_k being the resistance of k^{th} node.

In this VSI, the higher the value of VSI, the more stable the voltage stability in the microgrid system. Thus, for a minimization function, a deviation must be calculated. A voltage stability deviation index (dVSI) can be calculated as follow based on (Nguyen et al., 2016) as follows:

$$\Delta VSI = \max\left(\frac{1 - VSI_i}{1}\right) \quad \forall i = 2, \dots, N_{bus} \quad (28)$$

3.4.3 Power Loss And Voltage Stability Index

Then, the objective function is the minimization of total power loss and dVSI based on the paper by Nguyen et al. (2016). The equation is:

$$\text{minimize } F = \Delta P_{loss}^R + \Delta VSI \quad (29)$$

3.5 CUCKOO SEARCH ALGORITHM

In this research, the target of CSA simulation is to find the minimum value of the objective function, which is a total power loss and dVSI as a single objective. The simulation also was compared to a single objective of dVSI only and total power loss only to study the extent of the algorithm when dealing with two objectives as a single objective. Figure 3.6 shows the flowchart of microgrid reconfiguration by using CSA via Levy Flight. The steps of CSA in this research are:

- i. System data such as branch and bus number, busload, and resistance and reactance were loaded in the MATLAB program.
- ii. EV loads were added to microgrid to simulate application of EV loads integration to IEEE-33 and IEEE-69 microgrids.
- iii. Bus voltage magnitude and angles together with power loss (P_{loss}) are evaluated by executing the power flow program in MATLAB.
- iv. Initial configuration, which is before reconfiguration open switch set is defined as: $x_i = (x_i)_1^0 \cdots (x_i)_{n_e}^0$.
- v. The power loss before reconfiguration, x_i is calculated and denoted as P_{loss}^0 .
- vi. Algorithm parameters is configured such as tie switch dimension (n_e), nest dimension (n_d), number of nests (n), discoverability probability (p_a),

and step size (α), lower limit search space (l_a), upper limit search space (l_b) and maximum iteration number (N). In this research, both IEEE-33 and IEEE-69 bus system have the value n_e of 5. Value of n_d is 33 in IEEE-33 bus system and 69 in IEEE-69 bus system. Thus, n_d is the number of buses in the system. Number of nests (n) is 20 for both bus system, α is 0.25, l_a is always 1, l_b is the number of elements in fundamental loops that is not repeated in other fundamental loops. In IEEE-33, l_b is 7, 9, 4, 8, and 8 for fundamental loop one to five. Meanwhile, in IEEE-69 bus system, l_b is 12, 17, 13, 8, and 7. Number of iteration N is 40.

- vii. Search space $n \times n_d$ is randomly generated as initial population. Each row indicates a set of solution. Meanwhile, every element of x_c indicates sectionalizing switch of each solution.

$$x_c = \begin{pmatrix} (x_c)_1^1 & \cdots & (x_c)_{n_d}^1 \\ \vdots & \ddots & \vdots \\ (x_c)_1^n & \cdots & (x_c)_{n_d}^n \end{pmatrix} \quad (30)$$

- viii. Then, CSA is performed by using the Levy flight method to find potential solutions. The formula of Levy distribution is:

$$Levy \sim u = t^{-\lambda} \quad 1 < \lambda \leq 3 \quad (31)$$

Levy flight is a random walk based on Levy distribution. The formula for finding a new solution with Levy flight as is follows, while t is the current iteration number:

$$x_i^{(t+1)} = x_i^{(t)} + \alpha \oplus Levy(\lambda) \quad (32)$$

- ix. Then, the bus voltage of every element of x_c is calculated, and the real power loss after reconfiguration also were calculated denoted as $(P_{loss}^{rec})'$, for each element x_c .

- x. After that, real power loss reduction is calculated by:

$$(\Delta P_{loss}^R)' = \frac{(P_{loss}^{rec})'}{P_{loss}^0} \quad (33)$$

- xi. Then, dVSI was calculated for every element of x_c , and the maximum value was taken as dVSI value:

$$(\Delta VSI)' = \max\left(\frac{1 - VSI(x_c)_i}{1}\right) \quad \forall i = 2, \dots, N_d \quad (34)$$

xii. The value of power loss minimization ratio with dVSI is obtained by:

$$F' = \min((\Delta P_{loss}^R)' + (\Delta VSI)') \quad (35)$$

While F' is the minimum value for power loss reduction ratio and voltage stability for solution found by using the Levy Flight method.

xiii. The bus voltage is accepted if the bus voltage per unit value is within the limit of the restricted value, which is between V_{max} and V_{min} . V_{max} is 1.1 and V_{min} is 0.9. If it is not, then F' is set as infinity.

xiv. Then, a solution was selected randomly in nest x_c , denoted as $(x_c)_j$. The minimum value of objective function $(x_c)_j$ is denoted as F_j .

xv. If the solution selected by the Levy flight method was better, F' would replace F_i . Else, F_i is kept as a solution.

xvi. Then, rejected solution of p_a would be abandoned, and new solutions would be built by using the Levy Flight path.

xvii. The best solution would be preserved.

xviii. The solution would be ranked to find the best current solution.

xix. Iteration is increased by 1 and if it does not reach the maximum iteration number, repeat step xii. Else, go to step xix.

xx. The result would be displayed.

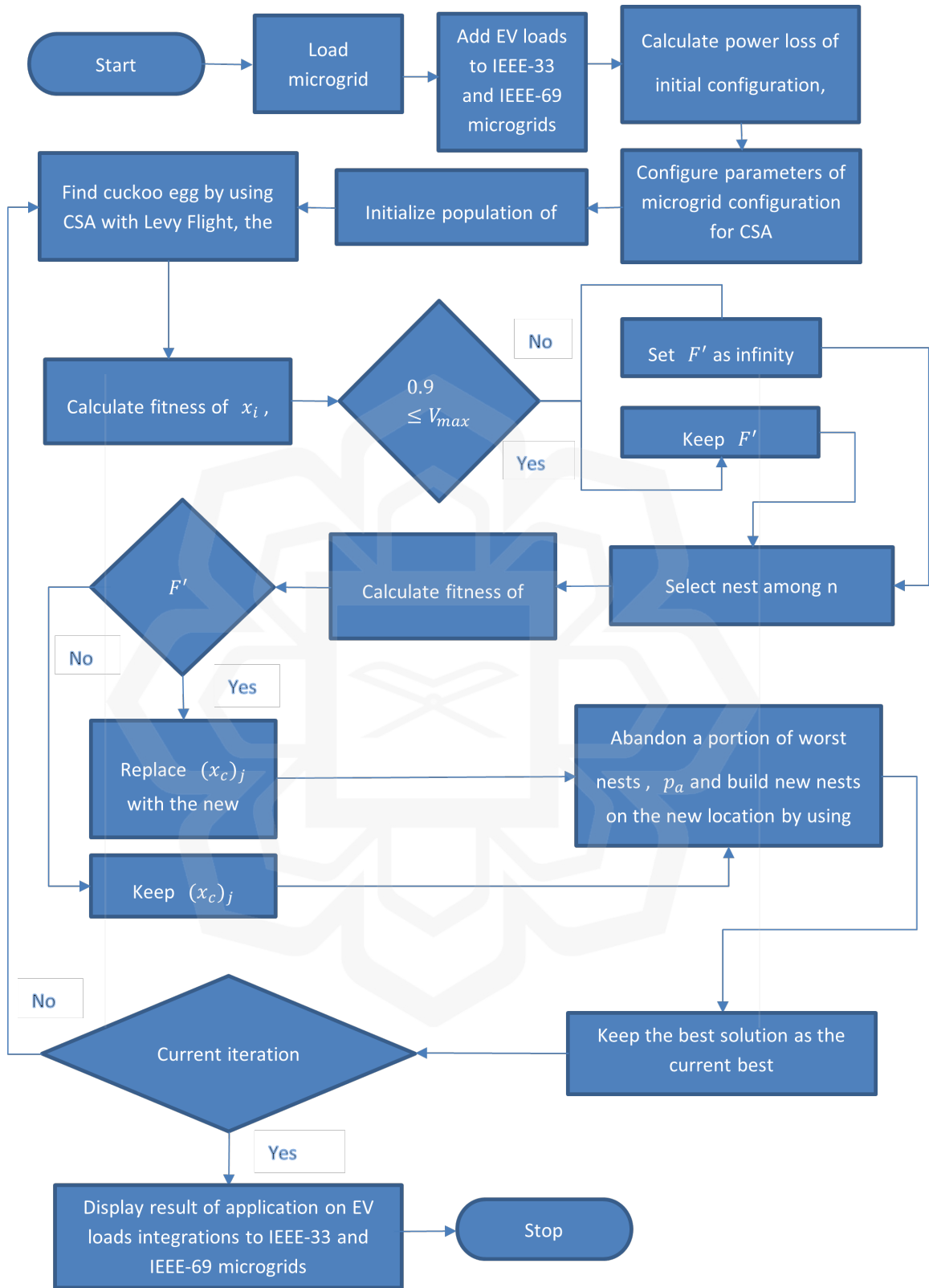
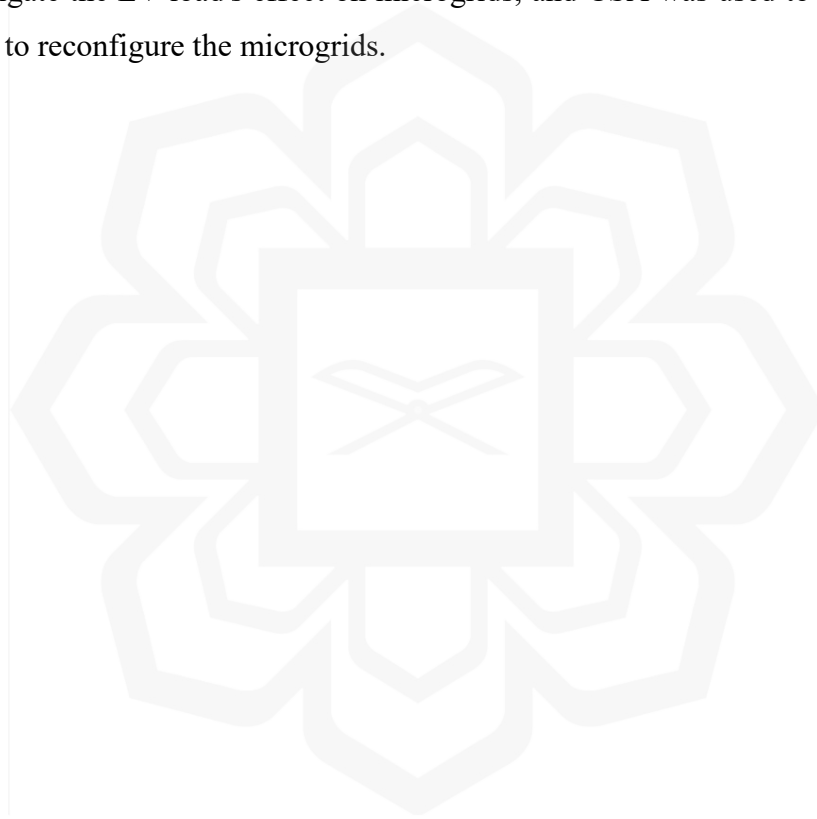


Figure 3.6: Flowchart of microgrid reconfiguration by using CSA via Levy Flight.

3.6 SUMMARY

In summary, the research methodology was designed to simulate the application of EV load integrations to IEEE-33 and IEEE-69 microgrids. IEEE-33 microgrids is an application for small-scale microgrids meanwhile IEEE-69 is an application for medium-scale microgrids. Both the strongest and weakest bus based on VSI were determined to find the effect of EV load integrations on microgrids. Thus, power loss and VSI can be calculated and analyzed to investigate the EV load's effect on microgrids, and CSA was used to find the extent of the CSA to reconfigure the microgrids.



CHAPTER FOUR

RESULTS AND DISCUSSIONS

4.1 OVERVIEW

In this chapter, the results and discussion are divided into two parts, subchapter 4.2 is for the IEEE-33 bus system representing small-scale microgrids, and subchapter 4.3 represents the IEEE-69 bus system representing medium-scale microgrids. Besides that, subchapters 4.2 and 4.3 are further divided into seven (7) index cases and analyses of the simulation results. Finally, subchapter 4.4 summarize this chapter's findings.

4.2 IEEE-33 BUS SYSTEM

In the IEEE-33 bus system, seven (7) index cases which are indicated as index 0 to 6, were simulated with EV charging load integration cases. Index 0 is the case when no EV charging load is connected to the microgrid. Index 1 is 1500kW EV charging load is connected to bus 2, index 2 is when 3000kW EV charging load is connected to bus 2 and index 3 is when 7500kW EV charging load is connected to bus 2. Index 1 to index 3 is when the EV charging load is connected to the strongest bus. Besides that, index 4, 3000kW charging load is connected to the bus system which is bus 2 and 19 each have 1500kW EV charging load. Index 5 is the situation when 1500kW EV charging load is connected to weakest bus which is bus 18. Lastly, index 6 is when 3000kW EV charging load is connected to the two weakest buses, bus 18 and bus 17, 1500kW for each bus.

4.2.1 Without EV Charging Load (Index 0)

In this case, no load from the EV charger is integrated into the microgrid. The result was shown in Table 4.1. When no EV charging load was integrated into the microgrid and only minimization of power loss is considered, CSA could reduce power loss higher than PSO and GA by 5.91 % and 0.21% respectively. While for VSI only, CSA gave a slightly better value than PSO and GA by 0.0130 and 0.0102 points respectively. When power loss and VSI are both considered as a single objective, CSA shows an objective function score better than PSO and GA by 0.0253 and 0.0095 points respectively. GA find a better power loss minimization by 0.21% but worse VSI by 0.0115 points compared to CSA but PSO is worse than CSA for both power loss minimization and VSI improvement. This shows CSA can find a better trade-off between power loss and voltage stability compared to PSO and GA in Index 0. Thus, the simulation shows CSA is better than GA followed by PSO when no EV charging load is integrated in microgrid.

Table 4.1: IEEE-33 for CSA Index 0

Scenario	Item	CSA	PSO	GA
Base Case	Switches opened	33 34 35 36 37		
	Power Loss (kW)	202.68		
	Min Voltage (p.u)	0.9131		
	Minimum VSI	0.6970		
Power Loss	Switches opened	7 9 14 32 37	7 14 32 35 37	7 9 14 28 32

	Power Loss (kW)	139.55	151.51	139.98
	% Loss Reduction	31.15	25.24	30.94
	Min Voltage (p.u)	0.9378	0.9360	0.9413
	Minimum VSI	0.7758	0.7687	0.7873
VSI	Switches opened	7 9 14 28 32	7 14 28 35 36	6 11 28 34 36
	Power Loss (kW)	139.98	152.37	150.43
	% Loss Reduction	30.94	24.82	25.78
	Min Voltage (p.u)	0.9413	0.9377	0.9386
	Minimum VSI	0.7873	0.7743	0.7771
Power Loss and VSI	Switches opened	7 9 14 28 32	7 11 32 34 37	7 9 14 32 37
	Power Loss (kW)	139.98	142.76	139.55
	% Loss Reduction	30.94	29.56	31.15
	Minimum Voltage (p.u)	0.9413	0.9378	0.9378
	Minimum VSI	0.7873	0.7758	0.7758
	Objective function score	0.9033	0.9286	0.9128

4.2.2 Index 1 in IEEE-33 Bus System

In Index 1, one (1) EV fast-charging load station is placed on bus 2 which is the strongest bus. In this case, a 1500 kW load is connected to the microgrid from EV chargers. The

result was shown in Table 4.2. When 1500 kW EV charging load was integrated into the microgrid and only minimization of power loss is considered, CSA could reduce power loss higher than PSO and GA by 8.81 % and 0.35% respectively. While for VSI only, CSA also gave a better value than PSO and GA by 0.0186 and 0.0126 points respectively. When power loss and VSI are both considered as a single objective, CSA shows an objective function score better than PSO and GA by 0.0247 and 0.0385 points respectively. CSA also is better than PSO and GA for both power loss minimization and VSI improvement when considered both as a single objective. This shows CSA can find the best solution for minimization of power loss and VSI improvement in Index 1 compared to PSO and GA. Thus, CSA can find the best microgrid configuration compared to PSO and GA when a 1500 kW EV charging load is integrated in microgrid.

Table 4.2: IEEE-33 for CSA Index 1

Scenario	Item	CSA	PSO	GA
Base Case	Switches opened	33 34 35 36 37		
	Power Loss (kW)	211.18		
	Min Voltage (p.u)	0.9121		
	Minimum VSI	0.6940		
Power Loss	Switches opened	7 9 14 32 37	7 17 28 34 35	7 10 14 32 37
	Power Loss (kW)	147.80	166.43	148.53
	% Loss Reduction	30.01	21.20	29.66
	Min Voltage (p.u)	0.9369	0.9318	0.9369
	Minimum VSI	0.7727	0.7552	0.7727

VSI	Switches opened	7 9 14 28 32	7 14 32 35 37	5 9 14 27 36
	Power Loss (kW)	148.23	159.81	172.19
	% Loss Reduction	29.81	24.32	18.47
	Min Voltage (p.u)	0.9404	0.9351	0.9369
	Minimum VSI	0.7842	0.7656	0.7716
Power Loss and VSI	Switches opened	7 9 14 28 32	7 11 32 34 37	6 11 34 36 37
	Power Loss (kW)	148.23	151.02	153.32
	% Loss Reduction	29.81	28.49	27.40
	Min Voltage (p.u)	0.9404	0.9369	0.9364
	Minimum VSI	0.7842	0.7727	0.7698
	Objective function	0.9177	0.9424	0.9562

4.2.3 Index 2 in IEEE-33 Bus System

In Index 2, two (2) EV fast-charging load stations are placed on bus 2 which is the strongest bus. In this case, a 3000 kW load is connected to the microgrid from EV chargers. The result was shown in Table 4.3. When 3000 kW EV charging load was integrated into the microgrid and only minimization of power loss is considered, CSA could reduce power loss higher than PSO and GA by 1.45 % and 4.04% respectively. While for VSI only, CSA also gave a better value than PSO and GA by 0.0186 and 0.0172 points respectively. When power loss and VSI are both considered as a single objective, CSA and GA show objective function score better than PSO by 0.0754 points. CSA and GA also are better than PSO for both power loss minimization and VSI improvement when considered both as a single

objective. This shows CSA and GA can find the best solution for minimization of power loss and VSI improvement in Index 2 compared to PSO. Thus, CSA and GA have the same result and can find a better configuration compared to PSO when the 3000 kW EV charging load is integrated into the microgrid.

Table 4.3: IEEE-33 for CSA Index 2

Scenario	Item	CSA	PSO	GA
Base Case	Switches opened	33 34 35 36 37		
	Power Loss (kW)	222.33		
	Min Voltage (p.u)	0.9112		
	Minimum VSI	0.6911		
Power Loss	Switches opened	7 9 14 32 37	7 11 32 34 37	6 9 14 28 32
	Power Loss (kW)	158.70	161.93	167.67
	% Loss Reduction	28.62	27.17	24.58
	Min Voltage (p.u)	0.9360	0.9360	0.9369
	Minimum VSI	0.7697	0.7697	0.7717
VSI	Switches opened	7 9 14 28 32	7 14 32 35 37	4 9 14 27 36
	Power Loss (kW)	159.13	170.76	187.93
	% Loss Reduction	28.43	23.20	15.47
	Min Voltage (p.u)	0.9394	0.9342	0.9343

	Minimum VSI	0.7812	0.7626	0.7640
Power Loss and VSI	Switches opened	7 9 14 28 32	7 14 32 35 37	7 9 14 28 32
	Power Loss (kW)	159.13	170.76	159.13
	% Loss Reduction	28.43	23.20	28.43
	Min Voltage (p.u)	0.9394	0.9342	0.9394
	Minimum VSI	0.7812	0.7626	0.7812
	Objective function	0.9346	1.01	0.9346

4.2.4 Index 3 in IEEE-33 Bus System

In Index 3, five (5) EV fast-charging load stations are placed on bus 2 which is the strongest bus. In this case, a 7500 kW load is connected to the microgrid from EV chargers. The result was shown in Table 4.4. When 7500 kW EV charging load was integrated into the microgrid and only minimization of power loss is considered, CSA and GA could reduce power loss higher than PSO by 1.21 %. While for VSI only, CSA gave a better value than PSO and GA by 0.0205 and 0.0100 points respectively. When power loss and VSI are both considered as a single objective, CSA shows an objective function score better than PSO and GA by 0.0613 and 0.0103 points respectively. GA find a better power loss minimization by 0.16% but worse VSI by 0.0114 points compared to CSA but PSO is worse than CSA for both power loss minimization and VSI improvement. This shows CSA can find a better trade-off between power loss and voltage stability compared to PSO and GA in index 3. Thus, the simulation shows CSA is better than GA followed by PSO when a 7500 kW EV charging load is integrated into the microgrid.

Table 4.4: IEEE-33 for CSA Index 3

Scenario	Item	CSA	PSO	GA
Base Case	Switches opened	33 34 35 36 37		
	Power Loss (kW)	271.78		
	Min Voltage (p.u)	0.9083		
	Minimum VSI	0.6824		
Power Loss	Switches opened	7 9 14 32 37	7 11 32 34 37	7 9 14 32 37
	Power Loss (kW)	207.39	210.66	207.39
	% Loss Reduction	23.70	22.49	23.70
	Min Voltage (p.u)	0.9332	0.9332	0.9332
	Minimum VSI	0.7605	0.7605	0.7605
VSI	Switches opened	7 9 14 28 32	3 8 14 17 28	6 11 28 34 36
	Power Loss (kW)	207.82	247.64	218.47
	% Loss Reduction	23.54	8.89	19.62
	Min Voltage (p.u)	0.9367	0.9306	0.9340
	Minimum VSI	0.7719	0.7514	0.7619
Power Loss and VSI	Switches opened	7 9 14 28 32	7 14 32 35 37	7 9 14 32 37
	Power Loss (kW)	207.82	219.58	207.39
	% Loss Reduction	23.54	19.21	23.70
	Min Voltage (p.u)	0.9367	0.9314	0.9332

	Minimum VSI	0.7719	0.7535	0.7605
	Objective function	0.9927	1.054	1.003

4.2.5 Index 4 in IEEE-33 Bus System

In Index 4, 1500kW EV fast-charging load is placed at bus 2 and bus 19 each. Thus, in this case, a 3000 kW load is connected to the microgrid from EV chargers. The result was shown in Table 4.5. When 3000 kW EV charging load was integrated into the microgrid and only minimization of power loss is considered at the two strongest buses, CSA and GA could reduce power loss higher than PSO by 5.38 %. While for VSI only, CSA gave a better value than PSO and GA by 0.0114 and 0.0101 points respectively. When power loss and VSI are both considered as a single objective, CSA shows an objective function score better than PSO and GA by 0.0240 and 0.0095 points respectively. GA find a better power loss minimization by 0.19% but worse VSI by 0.0114 points compared to CSA but PSO is worse than CSA for both power loss minimization and VSI improvement. This shows CSA can find a better trade-off between power loss and voltage stability compared to PSO and GA in Index 4. Thus, the simulation shows CSA is better than GA followed by PSO when the 3000 kW EV charging load is integrated into the microgrid to two (2) strongest buses.

Table 4.5: IEEE-33 for CSA Index 4

Scenario	Item	CSA	PSO	GA
Base Case	Switches opened	33 34 35 36 37		

	Power Loss (kW)	225.83		
	Min Voltage (p.u)	0.9112		
	Minimum VSI	0.6911		
Power Loss	Switches opened	7 9 14 32 37	7 14 32 35 37	7 9 14 32 37
	Power Loss (kW)	165.40	177.54	165.40
	% Loss Reduction	26.76	21.38	26.76
	Min Voltage (p.u)	0.9360	0.9325	0.9360
	Minimum VSI	0.7697	0.7572	0.7697
VSI	Switches opened	7 9 14 28 32	7 9 14 32 37	6 11 28 34 36
	Power Loss (kW)	165.83	165.38	176.86
	% Loss Reduction	26.57	26.76	21.68
	Min Voltage (p.u)	0.9394	0.9360	0.9368
	Minimum VSI	0.7811	0.7697	0.7710
Power Loss and VSI	Switches opened	7 9 14 28 32	7 11 32 34 37	7 9 14 32 37
	Power Loss (kW)	165.83	168.65	165.40
	% Loss Reduction	26.57	25.32	26.76
	Min Voltage (p.u)	0.9394	0.9360	0.9360
	Minimum VSI	0.7811	0.7697	0.7697
	Objective function	0.9532	0.9772	0.9627

4.2.6 Index 5 in IEEE-33 Bus System

In Index 5, one (1) EV fast-charging station is placed on bus 18 which is the weakest bus. In this case, a 1500 kW charging load is connected to the microgrid from the EV chargers to the weakest bus. The result was shown in Table 4.6. When 1500 kW EV charging load was integrated into the microgrid and only minimization of power loss is considered at the weakest bus, CSA and GA could reduce power loss higher than PSO by 1.54 %. While for VSI only, CSA and PSO gave better value than GA by 0.0094. When power loss and VSI are both considered as a single objective, CSA shows an objective function score better than PSO and GA by 0.0837 and 0.0467 respectively. CSA also is better than PSO and GA for both power loss minimization and VSI improvement when considered both as a single objective. This shows CSA can find the best solution for minimization of power loss and VSI improvement in index 5 compared to PSO and GA. Thus, CSA can find the best microgrid configuration compared to PSO and GA when a 1500 kW EV charging load is integrated into the microgrid's weakest bus.

Table 4.6: IEEE-33 for CSA Index 5

Scenario	Item	CSA	PSO	GA
Base Case	Switches opened	33 34 35 36 37		
	Power Loss (kW)	774.93		
	Min Voltage (p.u)	0.7609		
	Minimum VSI	0.3445		
Power Loss	Switches opened	7 9 14 17 28	7 17 28 34 35	7 9 14 17 28

	Power Loss (kW)	428.09	439.97	428.09
	% Loss Reduction	44.76	43.22	44.76
	Min Voltage (p.u)	0.8631	0.8630	0.8631
	Minimum VSI	0.5702	0.5701	0.5702
VSI	Switches opened	3 8 14 17 28	3 13 17 28 35	4 9 17 28 34
	Power Loss (kW)	451.68	471.63	443.34
	% Loss Reduction	41.71	39.14	42.79
	Min Voltage (p.u)	0.8659	0.8659	0.8653
	Minimum VSI	0.5776	0.5776	0.5761
Power Loss and VSI	Switches opened	7 9 14 17 28	13 17 20 28 35	7 9 14 16 28
	Power Loss (kW)	428.09	483.41	444.47
	% Loss Reduction	44.76	37.62	42.64
	Min Voltage (p.u)	0.8631	0.8584	0.8588
	Minimum VSI	0.5702	0.5580	0.5449
	Objective function	0.9823	1.066	1.029

4.2.7 Index 6 in IEEE-33 Bus System

In Index 6, one (1) EV fast-charging station is connected to bus 18 and bus 17 each. Thus, in this case, a 3000 kW load is connected to the microgrid from EV chargers. The initial configuration in this index has a voltage collapse condition as the VSI of the configuration

is below 0. The result was shown in Table 4.7. When 3000 kW EV charging load was integrated into the microgrid and only minimization of power loss is considered at the two (2) weakest buses, CSA could reduce power loss higher than PSO and GA by 0.04% and 0.03% respectively. While for VSI only, CSA also gave a better value than PSO and GA by 0.0300 and 0.0044 points respectively. When power loss and VSI are both considered as a single objective, CSA shows an objective function score better than PSO and GA by 0.1271 and 0.0157 respectively. CSA also is better than PSO and GA for both power loss minimization and VSI improvement when considered both as a single objective. This shows CSA can find the best solution for minimization of power loss and VSI improvement in Index 6 compared to PSO and GA. Thus, CSA can find the best microgrid configuration compared to PSO and GA when 3000 kW EV charging load integrated into microgrid two (2) weakest bus and all algorithms can find stable reconfiguration despite the initial configuration being collapsed and the calculation of power flow by using the N-R technique does not converge.

Table 4.7: IEEE-33 for CSA Index 6

Scenario	Item	CSA	PSO	GA
Base Case	Switches opened	33 34 35 36 37		
	Power Loss (kW)	134600.25		
	Min Voltage (p.u)	0.2617		
	Minimum VSI	-5.5718		
Power Loss	Switches opened	7 9 14 17 28	7 14 17 28 35	6 9 14 17 28
	Power Loss (kW)	718.62	767.03	750.27
	% Loss Reduction	99.47	99.43	99.44

	Min Voltage (p.u)	0.8517	0.8374	0.8414
	Minimum VSI	0.5668	0.5413	0.5513
VSI	Switches opened	7 10 14 17 28	11 14 17 20 28	7 9 14 17 27
	Power Loss (kW)	725.03	840.51	728.18
	% Loss Reduction	99.46	99.38	99.46
	Min Voltage (p.u)	0.8496	0.8422	0.8516
	Minimum VSI	0.5667	0.5367	0.5623
Power Loss and VSI	Switches opened	7 9 14 17 28	17 20 25 34 35	6 9 14 17 28
	Power Loss (kW)	718.62	995.50	750.27
	% Loss Reduction	99.47	99.26	99.44
	Min Voltage (p.u)	0.8517	0.7942	0.8414
	Minimum VSI	0.5668	0.4417	0.5513
	Objective function	0.4386	0.5657	0.4543

4.2.8 Analysis of PSO, GA, and CSA in IEEE-33 Bus System

Overall, CSA shows a better simulation result compared with GA and PSO. CSA also has a consistent result for all ten simulations for each index and scenario except for VSI only in index 5 as there is only one simulation that shows a worse result. Meanwhile, GA and PSO are less consistent to have the same result. PSO is the worst in all three simulation algorithms as PSO algorithm solution is easy to be trapped in local optima. Figure 4.1 shows the comparison of power loss between CSA, PSO, and GA in the IEEE-33 bus

system. Figure 4.2 shows the comparison of VSI between CSA, PSO, and GA in the IEEE-33 bus system. Figure 4.3 shows the score of objective function between CSA, PSO, and GA in the IEEE-33 bus system.

In conclusion, in the IEEE-33 bus system with EV charging load integration, CSA has the best result, especially when considering power loss and VSI as a single objective. Only index 2 CSA has the same result as GA. Besides that, GA is the second in terms of the best simulation result followed by PSO.

Thus, microgrid reconfiguration can reduce negative impacts on small-scale microgrids such as harmonic distortion, power loss, and equipment overloading when EV charging loads are integrated into the weakest and strongest bus in IEEE-33. By using CSA, a microgrid can be reconfigured better in terms of power loss and VSI compared to GA and PSO. As negative impacts on microgrids can be reduced, a microgrid is more reliable to cater to EV charging loads in the small-scale microgrid, consequently reducing carbon dioxide emission to the environment.

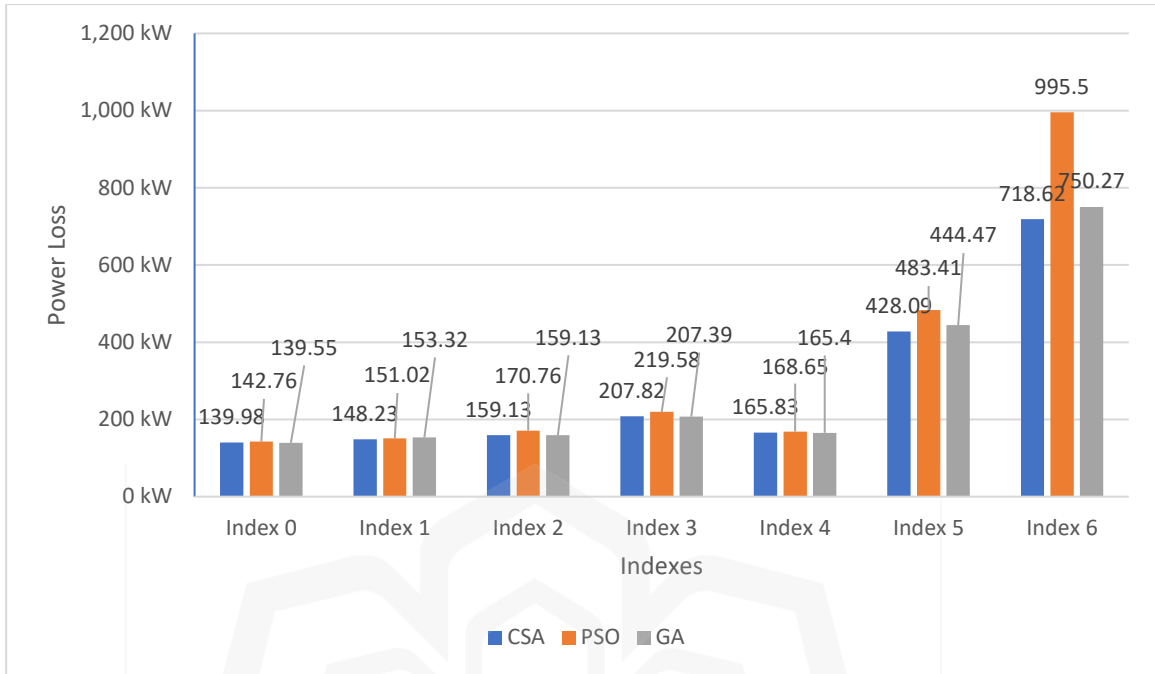


Figure 4.1: Comparison of power losses obtained by CSA, PSO, and GA for all cases in the IEEE-33 bus system.

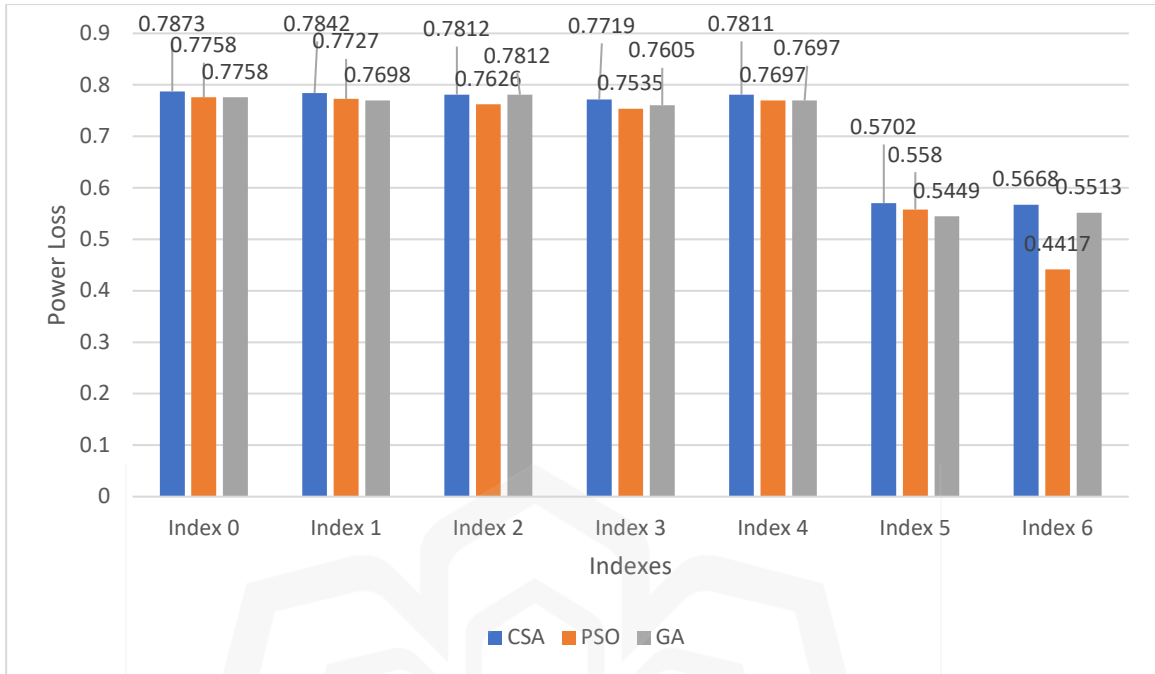


Figure 4.2: Comparison of VSI obtained by CSA, PSO, and GA for all cases in the IEEE-33 bus system.

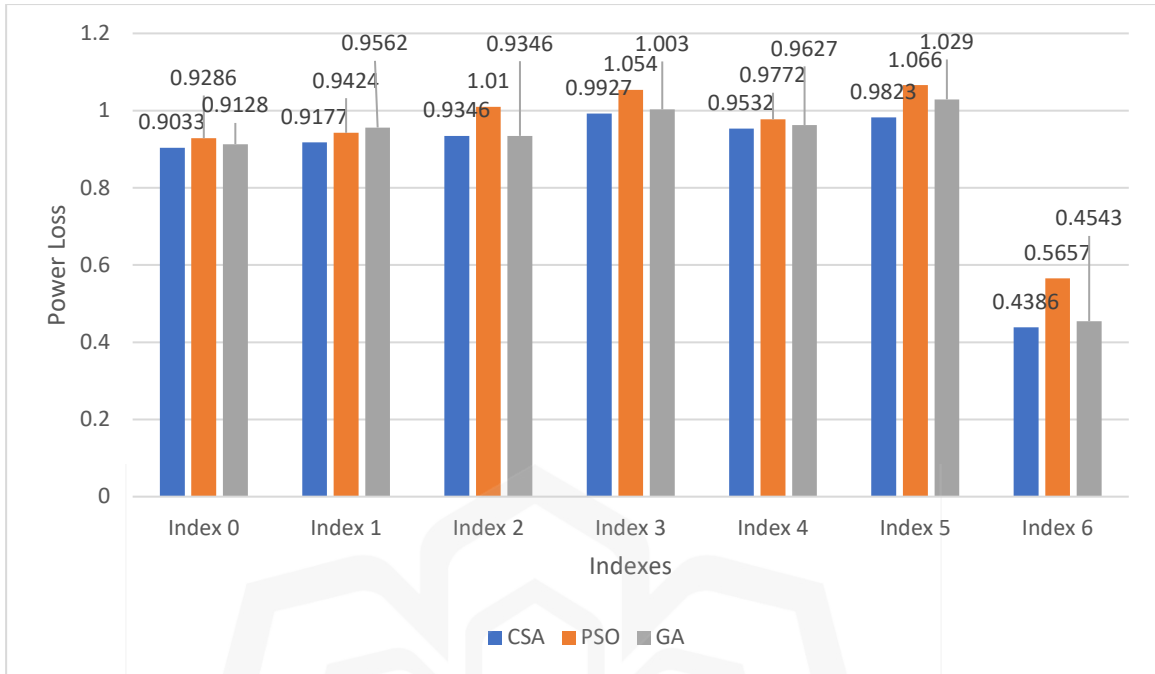


Figure 4.3: Comparison of objective function score between CSA, PSO, and GA for all cases in the IEEE-33 bus system.

4.3 IEEE-69 BUS SYSTEM

4.3.1 Without EV Charging Load (Index 0)

In this case, no load from the EV charger is integrated into the microgrid. The result was shown in Table 4.8. When no EV charging load was integrated into the microgrid and only minimization of power loss is considered, CSA could reduce power loss higher than PSO and GA by 7.68 % and 2.90% respectively. While for VSI only, CSA and GA gave better values than PSO by 0.0001 points. When power loss and VSI are both considered as a single objective, CSA shows an objective function score better than PSO and GA by 0.0762 and 0.0289 points respectively. CSA also is better than PSO and GA for power loss

minimization, but CSA and GA have the same VSI improvement and are better compared to PSO when considered both as a single objective. This shows CSA can find the best solution for minimization of power loss and VSI improvement as a single objective in Index 0 compared to PSO and GA. Thus, CSA can find the best microgrid configuration compared to PSO and GA when no EV charging load is integrated into the microgrid.

Table 4.8: IEEE-69 for CSA Index 0

Scenario	Item	CSA	PSO	GA
Base Case	Switches opened	69 70 71 72 73		
	Power Loss (kW)	224.98		
	Min Voltage (p.u)	0.9092		
	Minimum VSI	0.6850		
Power Loss	Switches opened	14 56 61 69 70	13 20 42 56 61	9 14 58 61 70
	Power Loss (kW)	99.61	116.76	106.13
	% Loss Reduction	55.73	48.10	52.83
	Min Voltage (p.u)	0.9428	0.9427	0.9428
	Minimum VSI	0.8085	0.8084	0.8085
VSI	Switches opened	5 14 56 61 70	13 20 42 58 61	4 14 56 61 70
	Power Loss (kW)	116.21	116.76	116.21

	% Loss Reduction	48.35	48.10	48.35
	Min Voltage (p.u)	0.9428	0.9427	0.9428
	Minimum VSI	0.8086	0.8084	0.8086
Power Loss and VSI	Switches opened	14 56 61 69 70	13 20 42 56 61	9 14 57 61 70
	Power Loss (kW)	99.61	116.76	106.13
	% Loss Reduction	55.73	48.10	52.83
	Min Voltage (p.u)	0.9428	0.9427	0.9428
	Minimum VSI	0.8085	0.8084	0.8085
	Objective function	0.6343	0.7105	0.6632

4.3.2 Index 1 in IEEE-69 Bus System

In Index 1, one (1) EV fast-charging load station is placed on bus 2 which is the strongest bus. In this case, a 1500 kW load is connected to the microgrid from EV chargers. The result was shown in Table 4.9. When 1500 kW EV charging load was integrated into the microgrid to the strongest bus and only minimization of power loss is considered, CSA could reduce power loss higher than PSO and GA by 7.62% and 3.56% respectively. While for VSI only, CSA and GA gave better values than PSO by 0.0001 points. When power loss and VSI are both considered as a single objective, CSA shows an objective function score better than PSO and GA by 0.0762 and 0.0252 points respectively. CSA also is better than PSO and GA for power loss minimization, but CSA and GA have the same VSI improvement and are better compared to PSO when considered both as a single objective. This shows CSA can find the best solution for minimization of power loss and VSI

improvement as a single objective in Index 1 compared to PSO and GA. Thus, CSA can find the best microgrid configuration compared to PSO and GA when a 1500 kW EV charging load is integrated into the microgrid to the strongest bus.

Table 4.9: IEEE-69 for CSA Index 1

Scenario	Item	CSA	PSO	GA
Base Case	Switches opened	69 70 71 72 73		
	Power Loss (kW)	225.03		
	Min Voltage (p.u)	0.9092		
	Minimum VSI	0.6850		
Power Loss	Switches opened	14 56 61 69 70	13 20 42 58 61	9 13 20 56 61
	Power Loss (kW)	99.66	116.80	107.68
	% Loss Reduction	55.71	48.09	52.15
	Min Voltage (p.u)	0.9428	0.9427	0.9428
	Minimum VSI	0.8085	0.8084	0.8085
VSI	Switches opened	5 14 56 61 70	13 20 42 56 61	9 14 56 61 70
	Power Loss (kW)	116.26	116.80	106.17
	% Loss Reduction	48.34	48.09	52.82
	Min Voltage (p.u)	0.9428	0.9427	0.9428

	Minimum VSI	0.8085	0.8084	0.8085
Power Loss and VSI	Switches opened	14 56 61 69 70	13 20 42 58 61	10 14 55 61 70
	Power Loss (kW)	99.65	116.80	105.35
	% Loss Reduction	55.71	48.09	53.19
	Minimum Voltage (p.u)	0.9428	0.9427	0.9428
	Min VSI	0.8085	0.8084	0.8085
	Objective function	0.6344	0.7106	0.6596

4.3.3 Index 2 in IEEE-69 Bus System

In Index 2, two (2) EV fast-charging load stations are placed on bus 2 which is the strongest bus. Thus, in this case, a 3000 kW load is connected to the microgrid from EV chargers. The result was shown in Table 4.10. When 3000 kW EV charging load was integrated into the microgrid and only minimization of power loss is considered, CSA could reduce power loss higher than PSO and GA by 6.58 % and 2.83% respectively. While for VSI only, CSA also gave a better value than PSO and GA by 0.0001 and 0.0231 points respectively. When power loss and VSI are both considered as a single objective, CSA shows an objective function score better than PSO and GA by 0.0763 and 0.0281 points respectively. CSA also is better than PSO and GA for both power loss minimization and VSI improvement when considered both as a single objective. This shows CSA can find the best solution for minimization of power loss and VSI improvement in Index 2 compared to PSO and GA.

Thus, CSA can find the best microgrid configuration compared to PSO and GA when a 3000 kW EV charging load is integrated into the microgrid to the strongest bus.

Table 4.10: IEEE-69 for CSA Index 2

Scenario	Item	CSA	PSO	GA
Base Case	Switches opened	69 70 71 72 73		
	Power Loss (kW)	225.09		
	Min Voltage (p.u)	0.9092		
	Minimum VSI	0.6850		
Power Loss	Switches opened	14 57 61 69 70	10 17 45 58 61	10 14 56 63 70
	Power Loss (kW)	99.71	114.51	106.09
	% Loss Reduction	55.70	49.12	52.87
	Min Voltage (p.u)	0.9427	0.9428	0.9414
	Minimum VSI	0.8085	0.8085	0.7854
VSI	Switches opened	5 14 58 61 70	13 20 42 58 61	4 14 57 63 70
	Power Loss (kW)	116.32	116.86	116.72
	% Loss Reduction	48.33	48.08	48.15
	Min Voltage (p.u)	0.9428	0.9427	0.9414

	Minimum VSI	0.8085	0.8084	0.7854
Power Loss and VSI	Switches opened	14 55 61 69 70	13 20 42 58 61	13 57 62 69 70
	Power Loss (kW)	99.71	116.86	100.86
	% Loss Reduction	55.70	48.08	55.19
	Min Voltage (p.u)	0.9427	0.9427	0.9414
	Minimum VSI	0.8085	0.8084	0.7855
	Objective function	0.6345	0.7108	0.6626

4.3.4 Index 3 in IEEE-69 Bus System

In Index 3, five (5) EV fast-charging load stations are placed on bus 2 which is the strongest bus. Thus, in this case, a 7500 kW load is integrated into the microgrid grid from EV chargers. The result was shown in Table 4.11. When 7500 kW EV charging load was integrated into the microgrid and only minimization of power loss is considered, CSA and PSO could reduce power loss higher than GA by 2.53%. While for VSI only, CSA and GA have better value than PSO by 0.0002. When power loss and VSI are both considered as a single objective, CSA shows an objective function score better than PSO and GA by 0.0762 and 0.0252 points respectively. CSA also is better than PSO and GA for both power loss minimization and VSI improvement when considered both as a single objective. This shows CSA can find the best solution for minimization of power loss, but GA is better than CSA and PSO for VSI improvement in Index 3 when considering both as a single objective. Thus, CSA can find the best trade-off microgrid configuration compared to PSO and GA when a 7500 kW EV charging load is integrated into the microgrid to the strongest bus.

Table 4.11: IEEE-69 for CSA Index 3

Scenario	Item	CSA	PSO	GA
Base Case	Switches opened	69 70 71 72 73		
	Power Loss (kW)	225.36		
	Min Voltage (p.u)	0.9092		
	Minimum VSI	0.6850		
Power Loss	Switches opened	14 55 61 69 70	14 58 61 69 70	10 14 58 61 70
	Power Loss (kW)	99.97	99.97	105.66
	% Loss Reduction	55.64	55.64	53.11
	Min Voltage (p.u)	0.9427	0.9427	0.9427
	Minimum VSI	0.8084	0.8084	0.8085
VSI	Switches opened	4 14 55 61 70	18 42 45 56 61	4 13 20 57 61
	Power Loss (kW)	116.58	122.58	119.44
	% Loss Reduction	48.27	45.61	47.00
	Min Voltage (p.u)	0.9427	0.9427	0.9427
	Minimum VSI	0.8085	0.8083	0.8085

Power Loss and VSI	Switches opened	14 55 61 69 70	13 20 42 58 61	10 14 55 61 70
	Power Loss (kW)	99.97	117.12	105.66
	% Loss Reduction	55.64	48.03	53.11
	Min Voltage (p.u)	0.9427	0.9427	0.9427
	Minimum VSI	0.8084	0.8084	0.8085
	Objective function	0.6352	0.7114	0.6604

4.3.5 Index 4 in IEEE-69 Bus System

In Index 4, 1500kW EV charging loads are connected to bus 2 and bus 3 each. In this case, a 3000 kW load is connected to the microgrid from EV chargers to two (2) strongest buses. The result was shown in Table 4.12. When 1500 kW EV charging load was integrated into the microgrid and only minimization of power loss is considered, CSA and PSO could reduce power loss higher than PSO and GA by 2.56 %. Meanwhile, in VSI improvement only, CSA and GA have a better value than PSO by 0.0001. When power loss and VSI are both considered as a single objective, CSA shows an objective function score better than PSO and GA by 0.0762 and 0.0252 points respectively. CSA also is better than PSO and GA for power loss minimization, but CSA and GA have the same VSI improvement which is better than PSO in the objective function. This shows CSA can find the best solution for minimization of power loss among all algorithms but have the same result as GA for VSI improvement. Thus, CSA can find the best microgrid configuration for objective function compared to PSO and GA when the 3000 kW EV charging load is integrated into the microgrid to the strongest bus.

Table 4.12: IEEE-69 for CSA Index 4

Scenario	Item	CSA	PSO	GA
Base Case	Switches opened	69 70 71 72 73		
	Power Loss (kW)	225.14		
	Min Voltage (p.u)	0.9092		
	Minimum VSI	0.6850		
Power Loss	Switches opened	14 58 61 69 70	14 58 61 69 70	10 13 55 61 70
	Power Loss (kW)	99.76	99.76	105.52
	% Loss Reduction	55.69	55.69	53.13
	Min Voltage (p.u)	0.9427	0.9427	0.9428
	Minimum VSI	0.8085	0.8085	0.8085
VSI	Switches opened	5 14 55 61 70	13 20 42 58 61	4 13 20 56 61
	Power Loss (kW)	116.36	116.91	119.22
	% Loss Reduction	48.32	48.07	47.04
	Min Voltage (p.u)	0.9428	0.9427	0.9428
	Minimum VSI	0.8085	0.8084	0.8085

Power Loss and VSI	Switches opened	14 58 61 69 70	13 20 42 58 61	10 14 57 61 70
	Power Loss (kW)	99.76	116.90	105.45
	% Loss Reduction	55.69	48.07	53.16
	Min Voltage (p.u)	0.9427	0.9427	0.9428
	Minimum VSI	0.8085	0.8083	0.8085
	Objective function score	0.6347	0.7109	0.6599

4.3.6 Index 5 in IEEE-69 Bus System

In Index 5, one EV fast-charging load station is placed at bus 65 which is the weakest bus. In this case, a 1500 kW load is connected to the microgrid from EV chargers. The result was shown in Table 4.13. When 1500 kW EV charging load to the weakest bus was integrated into the microgrid and only minimization of power loss is considered, CSA could reduce power loss higher than PSO and GA by 6.10 % and 3.45% respectively. While for VSI only, CSA also gave a better value than PSO and GA by 0.038 and 0.109 points respectively. When power loss and VSI are both considered as a single objective, CSA shows an objective function score better than PSO and GA by 0.1053 and 0.1245 points respectively. CSA also is better than PSO and GA for both power loss minimization and VSI improvement when considered both as a single objective. This shows CSA can find the best solution for minimization of power loss and VSI improvement in index 5 compared to PSO and GA. Thus, CSA can find the best microgrid configuration compared to PSO and GA when a 1500 kW EV charging load is integrated into the microgrid to the weakest bus.

Table 4.13: IEEE-69 for CSA Index 5

Scenario	Item	CSA	PSO	GA
Base Case	Switches opened	69 70 71 72 73		
	Power Loss (kW)	692.30		
	Min Voltage (p.u)	0.8168		
	Minimum VSI	0.4700		
Power Loss	Switches opened	14 56 64 69 70	10 20 45 56 64	13 20 58 64 69
	Power Loss (kW)	266.91	309.10	290.78
	% Loss Reduction	61.45	55.35	58.00
	Min Voltage (p.u)	0.9126	0.8980	0.9073
	Minimum VSI	0.7275	0.6832	0.7114
VSI	Switches opened	14 56 64 69 70	20 45 58 64 69	13 20 42 52 63
	Power Loss (kW)	266.91	321.58	349.76
	% Loss Reduction	61.45	53.55	49.48
	Min Voltage (p.u)	0.9126	0.9002	0.8844
	Minimum VSI	0.7275	0.6897	0.6181

Power Loss and VSI	Switches opened	14 56 64 69 70	10 20 45 58 64	14 58 63 69 70
	Power Loss (kW)	266.91	309.10	293.61
	% Loss Reduction	61.45	55.35	57.59
	Min Voltage (p.u)	0.9126	0.8980	0.8928
	Minimum VSI	0.7275	0.6832	0.6416
	Objective function	0.6580	0.7633	0.7825

4.3.7 Index 6 in IEEE-69 Bus System

In Index 6, two (2) 1500kW EV fast-charging loads are placed at bus 65 and bus 64. Those buses are the weakest bus in the system. In this case, a 3000 kW load is connected to the microgrid from EV chargers. The result was shown in Table 4.14. When 3000 kW EV charging load to the two (2) weakest buses was integrated into the microgrid and only minimization of power loss is considered, CSA could reduce power loss higher than PSO and GA by 3.35 % and 0.94% respectively. Interestingly, when considering VSI only, all algorithms show the same VSI improvement. When power loss and VSI are both considered as a single objective, CSA shows an objective function score better than PSO and GA by 0.0449 and 0.0134 points respectively. CSA also is better than PSO and GA for both power loss minimization, but GA is the best in VSI improvement when considered both as a single objective. This shows CSA can find the best solution for objective function in index 6 compared to PSO and GA. Thus, CSA can find the best microgrid configuration compared to PSO and GA when the 3000 kW EV charging load is integrated into the microgrid to the two (2) weakest buses.

Table 4.14: IEEE-69 for CSA Index 6

Scenario	Item	CSA	PSO	GA
Base Case	Switches opened	69 70 71 72 73		
	Power Loss (kW)	1757.59		
	Min Voltage (p.u)	0.7081		
	Minimum VSI	0.2695		
Power Loss	Switches opened	14 55 64 69 70	20 42 45 58 64	10 14 56 64 70
	Power Loss (kW)	493.90	552.69	510.46
	% Loss Reduction	71.90	68.55	70.96
	Min Voltage (p.u)	0.8796	0.8796	0.8796
	Minimum VSI	0.6221	0.6220	0.6222
VSI	Switches opened	5 14 57 64 70	4 14 55 64 70	4 14 55 64 70
	Power Loss (kW)	529.20	529.20	529.20
	% Loss Reduction	69.89	69.89	69.89
	Min Voltage (p.u)	0.8797	0.8797	0.8797
	Minimum VSI	0.6222	0.6222	0.6222
Power Loss and VSI	Switches opened	14 55 64 69 70	14 42 56 64 70	10 13 20 58 64

	Power Loss (kW)	493.90	572.60	517.50
	% Loss Reduction	71.90	67.42	70.56
	Min Voltage (p.u)	0.8796	0.8796	0.8796
	Minimum VSI	0.6221	0.6220	0.6222
	Objective function	0.6589	0.7038	0.6723

4.3.8 Analysis of PSO, GA, and CSA in IEEE-69 Bus System

In the analysis of reconfiguration in the IEEE-69 bus system, CSA also shows a better simulation result compared with GA and PSO. CSA also has a consistent result for every simulation index compared to GA and PSO. GA is the second most consistent algorithm in this research. PSO is the worst in all three simulation algorithms as PSO algorithm solution is easy to be trapped in local optima. Figure 4.4 shows the comparison of power loss of objective function between CSA, PSO, and GA in the IEEE-69 bus system. Figure 4.5 shows the comparison of VSI of objective function between CSA, PSO, and GA in the IEEE-69 bus system. Figure 4.6 shows the power loss and VSI as a single objective, which is the objective function between CSA, PSO, and GA in the IEEE-69 bus system.

In other words, in the IEEE-69 bus system with EV charging load integration, CSA has the best result in power loss and VSI as a single objective in all seven indexes. GA is the second in terms of the best simulation result followed by PSO because GA is better than PSO in six indexes which are index 0, 1, 2, 3, 4, and 6. Meanwhile, PSO is only better than GA in index 5 when dealing with power loss and VSI as a single objective.

Thus, microgrid reconfiguration can reduce negative impacts on medium-scale microgrids such as harmonic distortion, power loss, and equipment overloading when EV charging loads are integrated into the weakest and strongest bus in IEEE-69. By using CSA, a microgrid can be reconfigured better in terms of power loss and VSI compared to GA and PSO. As negative impacts on microgrids can be reduced, a microgrid is more reliable to cater to EV charging loads in the medium-scale microgrid, consequently reducing carbon dioxide emission to the environment.

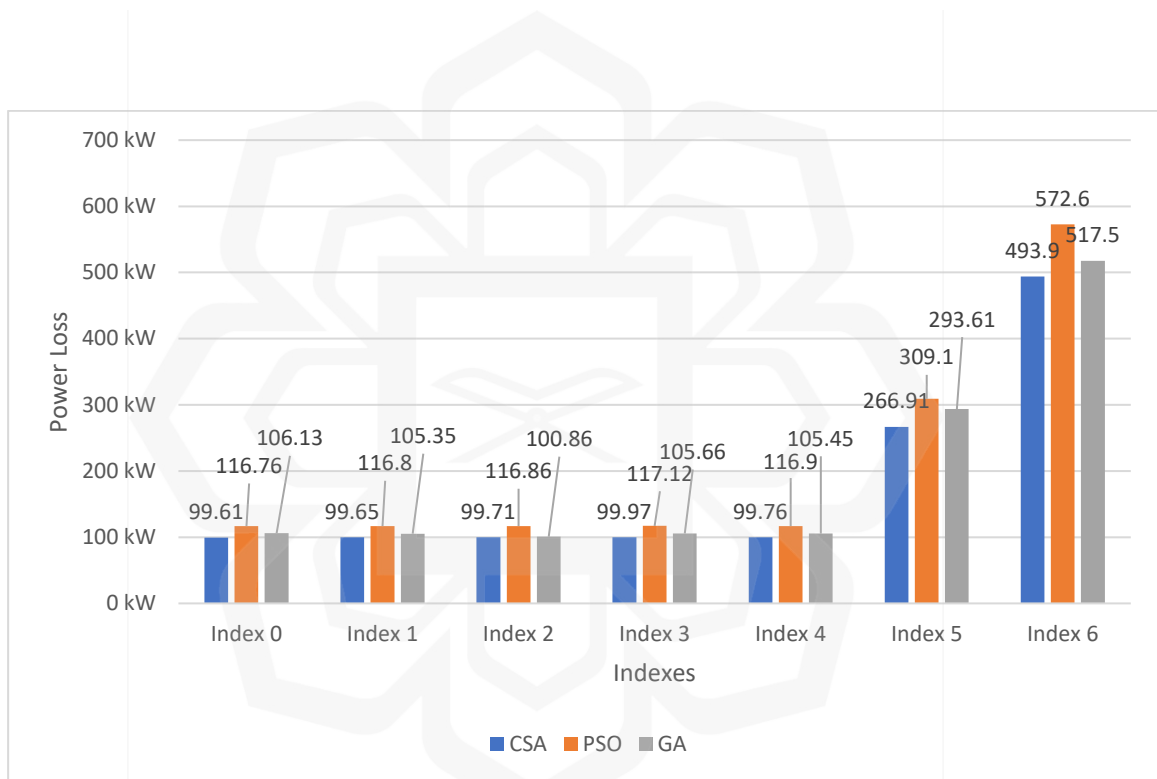


Figure 4.4: Comparison of power loss obtained between CSA, PSO, and GA for all cases in the IEEE-69 bus system.

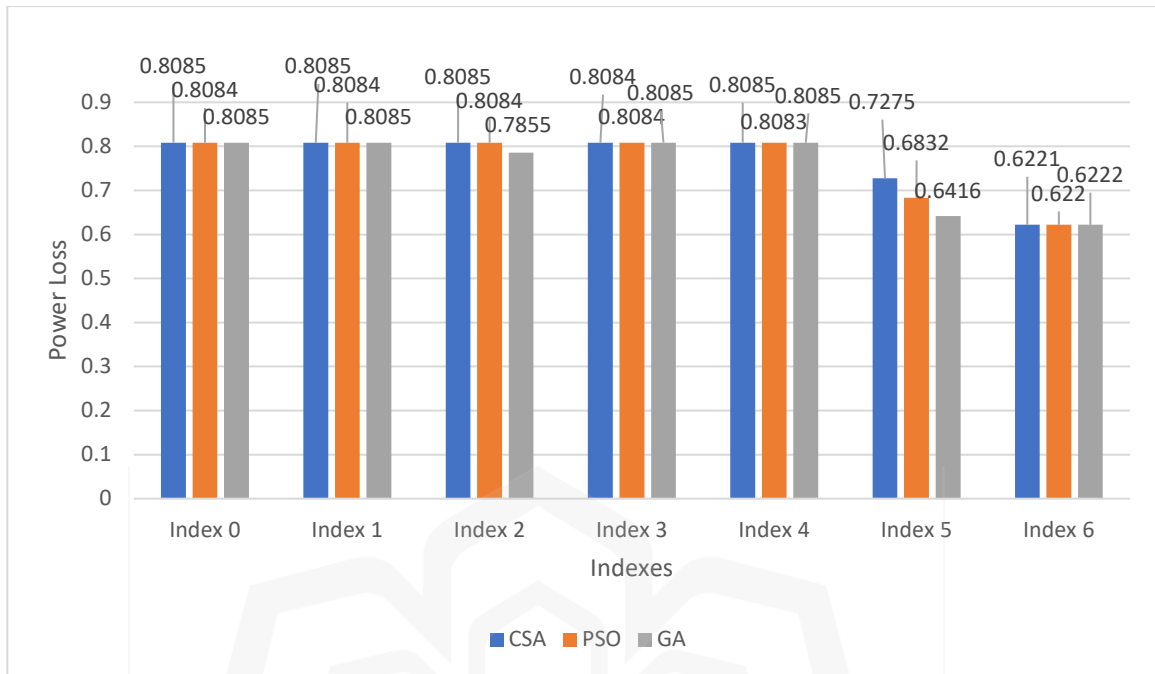


Figure 4.5: Comparison of VSI between CSA, PSO, and GA for all cases in the IEEE-69 bus system.

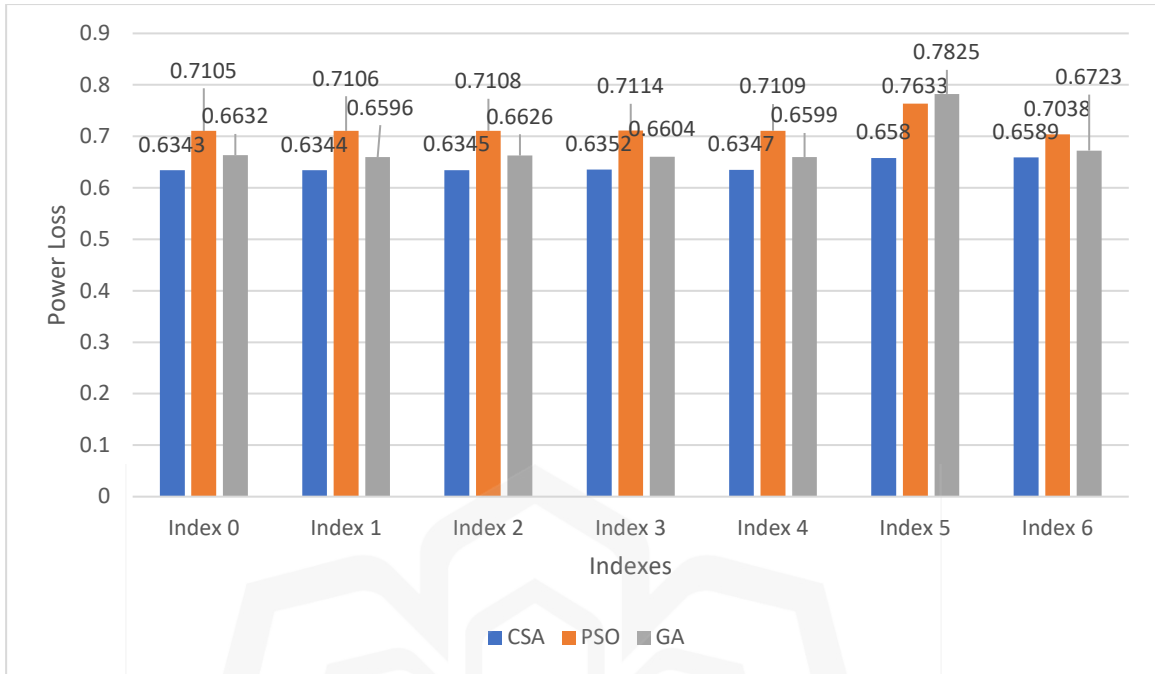


Figure 4.6: Comparison of objective function score between CSA, PSO, and GA for all cases in the IEEE-69 bus system.

4.4 SUMMARY

In conclusion, CSA can find a better microgrid reconfiguration with EV charging load integration compared to GA and PSO. CSA is also more consistent to find solutions compared to other algorithms. CSA also can find a better solution due to the Levy flight pattern to find a solution with Levy distribution elementwise to the potential candidates. GA is the second-best among these algorithms followed by PSO. PSO is the worst as PSO is easily trapped to local optima. In index 6 of the IEEE-33 bus system, all three algorithms can find a stable VSI configuration in the microgrid from the initial collapse configuration EV charging load is integrated into the two weakest buses. Thus, CSA, GA, and PSO can solve a microgrid reconfiguration problem with power loss and VSI as a single objective function, but CSA is the best among these algorithms.

CHAPTER FIVE

CONCLUSION

5.1 CONCLUSION

To combat global warming, carbon emissions must be reduced worldwide. To realize the effort, governments around the world like China and UK are replacing ICE by putting more EVs on the road to reduce carbon emissions in the transportation sector. But EV charging loads are causing a power loss and voltage instability to the microgrid. To make matter worse, charging activities also increase peak load, cause harmonic distortion, and equipment overloading. Thus, reconfiguration of the microgrid is needed. To optimize the network reconfiguration, an algorithm is needed to find the best configuration. CSA is the algorithm in this research to discover the best microgrid configuration in respect of power loss and VSI as a single objective. CSA is chosen as the CSA is simple and does not have many parameters compared to PSO and GA.

In this research, the impact of EV charging load on microgrids is assessed. The finding is EV charging load increases power loss and reduces voltage stability. At some point, in the IEEE-33 bus system, voltage stability collapsed after charging loads were integrated into the two weakest buses. After that, an optimum reconfigurable microgrid for minimizing power losses and increasing voltage stability by using CSA is developed. CSA also performs better compared to PSO and GA. The optimum reconfigurable microgrid is done on the IEEE-33 bus system, which is a small-scale microgrid. Finally, the reconfigurable microgrid was applied to the medium-scale microgrid of the power distribution network. In this research, the finding is CSA is better to find better network reconfigurations compared to PSO and GA for medium-scale power distribution networks.

The reconfiguration on the medium scale is done on the IEEE-69 bus system and the reconfiguration is successful to find power loss reduction and voltage stability as a single objective. Thus, this reconfiguration model by using CSA can be applied to the medium-scale microgrid.

In the IEEE-33 bus system, which is the application on a small-scale microgrid, the objective function of CSA from Index 0 to Index 6 is better by between 0.0240 to 0.1271 points compared to PSO and between 0.0000 to 0.0467 compared to GA. Thus, when considering the balance between power loss reduction and VSI, CSA has the best simulation result in the IEEE-33 bus system except for Index 3 where CSA and GA have the same objective function value. This is followed by GA as the algorithm is better than PSO but worse than CSA. Lastly, PSOs have the worse objective function in all indexes.

In the IEEE-69 bus system which is the application on a medium-scale microgrid, the objective function of CSA from Index 0 to Index 6 is better by between 0.0449 to 0.1053 points compared to PSO and between 0.0134 to 0.1245 compared to GA. In other words, when considering the balance between power loss reduction and VSI, CSA has the best simulation result in the IEEE-69 bus system in all indexes. This is followed by GA as the algorithm is better than PSO in all indexes except index 5 which is PSO is better than GA.

Finally, it can be concluded that all three algorithms can find a better configuration compared to the initial configuration. But CSA is the best among these algorithms in power loss reduction and has the highest VSI as a single objective. Thus, CSA can be used to solve the problem of EV charging load into a microgrid reconfiguration. As power loss and VSI can be improved by using microgrid reconfiguration, stability and reliability of small-scale and medium-scale microgrids can be improved with EV charging loads integrated into microgrids' system. Carbon dioxide emission is reduced and one factor of global warming

can be reduced and potentially solved as the world are moving to EV in transportation sector.

5.2 LIMITATIONS AND FUTURE WORK

There are a few limitations to this research. In the future, this research can be expanded to a larger scale bus system model such as the IEEE-118 bus system to find CSA performance in terms to find the best solution compared to GA and PSO. Besides that, future research also can implement an improved version of the CSA algorithm such as by using the ACSA which is using Graph Theory to be compared to CSA, PSO, and GA. Furthermore, multi-objective CSA also can be investigated to find a Pareto optimum between power loss and VSI in a bus system.

REFERENCES

- Abdolahi, A., Salehi, J., Samadi Gazijahani, F., & Safari, A. (2018). Probabilistic multi-objective arbitrage of dispersed energy storage systems for optimal congestion management of active distribution networks including solar/wind/CHP hybrid energy system. *Journal of Renewable and Sustainable Energy*, 10(4). <https://doi.org/10.1063/1.5035081>
- Ahmed, A., Iqbal, A., Khan, I., Al-Wahedi, A., Mehrjerdi, H., & Rahman, S. (2021). Impact of EV charging Station Penetration on Harmonic Distortion Level in Utility Distribution Network: A Case Study of Qatar. *2021 IEEE Texas Power and Energy Conference, TPEC 2021*, 1–6. <https://doi.org/10.1109/TPEC51183.2021.9384952>
- Albadi, M. (2020). Power Flow Analysis. In *Computational Models in Engineering* (p. 13). IntechOpen. <https://doi.org/10.5772/intechopen.83374>
- Ali, E. M., Abdelsalam, A. K., Youssef, K. H., & Hossam-Eldin, A. A. (2021). An enhanced cuckoo search algorithm fitting for photovoltaic systems' global maximum power point tracking under partial shading conditions. *Energies*, 14(21). <https://doi.org/10.3390/en14217210>
- Arango Castellanos, J. D., Dhanasekaran Velayutha Rajan, H., Rohde, A. K., Denhof, D., & Freitag, M. (2019). Design and simulation of a control algorithm for peak-load shaving using vehicle to grid technology. *SN Applied Sciences*, 1(9), 1–12. <https://doi.org/10.1007/s42452-019-0999-x>
- Babalola, A. E., Ojokoh, B. A., & Odili, J. B. (2020). A Review of Population-Based Optimization Algorithms. *2020 International Conference in Mathematics, Computer Engineering and Computer Science, ICMCECS 2020*. <https://doi.org/10.1109/ICMCECS47690.2020.240856>

- Baran, M. E., & Wu, F. F. (1989). Network reconfiguration in distribution systems for loss reduction and load balancing. *IEEE Transactions on Power Delivery*, 4(2), 1401–1407. <https://doi.org/10.1109/61.25627>
- Barrero-González, F., Milanés-Montero, M. I., González-Romera, E., Romero-Cadaval, E., & Roncero-Clemente, C. (2019). Control strategy for electric vehicle charging station power converters with active functions. *Energies*, 12(20). <https://doi.org/10.3390/en12203971>
- Chen, T. H., & Liao, R. N. (2013). Analysis of charging demand of electric vehicles in residential area. *International Conference on Remote Sensing, Environment and Transportation Engineering, RSETE 2013, May 2016*, 27–31. <https://doi.org/10.2991/rsete.2013.7>
- Chiang, H.-D., & Jean-Jumeau, R. (1990). Optimal network reconfigurations in distribution systems. II. Solution algorithms and numerical results. *IEEE Transactions on Power Delivery*, 5(3), 1568–1574. <https://doi.org/10.1109/61.58002>
- Danish, M. S. S., Senjyu, T., Danish, S. M. S., Sabory, N. R., Narayanan, K., & Mandal, P. (2019). A recap of voltage stability indices in the past three decades. *Energies*, 12(8), 1–18. <https://doi.org/10.3390/en12081544>
- Deb, S., Kalita, K., & Mahanta, P. (2018). Impact of electric vehicle charging stations on reliability of distribution network. *Proceedings of 2017 IEEE International Conference on Technological Advancements in Power and Energy: Exploring Energy Solutions for an Intelligent Power Grid, TAP Energy 2017, 1*, 1–6. <https://doi.org/10.1109/TAPENERGY.2017.8397272>
- Deb, S., Tammi, K., Kalita, K., & Mahanta, P. (2018). Impact of Electric Vehicle Charging Station Load on Distribution Network. *Energies*. <https://doi.org/10.3390/en11010178>
- Dharmakeerthi, C. H., Mithulananthan, N., & Saha, T. K. (2014). Impact of electric vehicle fast charging on power system voltage stability. *International Journal of Electrical*

Power and Energy Systems, 57, 241–249. <https://doi.org/10.1016/j.ijepes.2013.12.005>

Di Silvestre, M. L., Riva Sanseverino, E., Zizzo, G., & Graditi, G. (2013). An optimization approach for efficient management of EV parking lots with batteries recharging facilities. *Journal of Ambient Intelligence and Humanized Computing*, 4(6), 641–649. <https://doi.org/10.1007/s12652-013-0174-y>

Fan, Y., Guo, C., Hou, P., & Tang, Z. (2013). Impact of Electric Vehicle Charging on Power Load Based on TOU Price. *Energy and Power Engineering*, 05(04), 1347–1351. <https://doi.org/10.4236/epe.2013.54b255>

Gao, Y., Gao, X., & Zhang, X. (2017). The 2 °C Global Temperature Target and the Evolution of the Long-Term Goal of Addressing Climate Change—From the United Nations Framework Convention on Climate Change to the Paris Agreement. *Engineering*, 3(2), 272–278. <https://doi.org/10.1016/J.ENG.2017.01.022>

Horton, B. P., Khan, N. S., Cahill, N., Lee, J. S. H., Kemp, A. C., Engelhart, S. E., Rahmstorf, S., Shaw, T. A., & Garner, A. J. (2005). Estimating global mean sea-level rise and its uncertainties by 2100 and 2300 from an expert survey. *Npj Climate and Atmospheric Science*, 1–8. <https://doi.org/10.1038/s41612-020-0121-5>

Immanuel, S. D., & Chakraborty, U. K. (2019). Genetic Algorithm: An Approach on Optimization. *Proceedings of the 4th International Conference on Communication and Electronics Systems, ICCES 2019, Icces*, 701–708. <https://doi.org/10.1109/ICCES45898.2019.9002372>

Jiang, C., Torquato, R., Salles, D., & Xu, W. (2014). Method to assess the power quality impact of plug-in electric vehicles. *Proceedings of International Conference on Harmonics and Quality of Power, ICHQP*, 29(2), 177–180. <https://doi.org/10.1109/ICHQP.2014.6842835>

Kementerian Perdagangan Antarabangsa dan Industri. (n.d.). Retrieved January 16, 2022, from <https://www.miti.gov.my/index.php/pages/view/nap2020>

- Kennedy, J., & Eberhart, R. (2010). Particle swarm optimization. *Proceedings of ICNN'95 - International Conference on Neural Networks*, 4, 1942–1948. <https://doi.org/10.1109/ICNN.1995.488968>
- Kongjeen, Y., & Bhumkittipich, K. (2018). Impact of plug-in electric vehicles integrated into power distribution system based on voltage-dependent power flow analysis. *Energies*, 11(6), 1–16. <https://doi.org/10.3390/en11061571>
- Kumar, J., Agarwal, A., & Agarwal, V. (2019). A review on overall control of DC microgrids. *Journal of Energy Storage*, 21, 113–138. <https://doi.org/10.1016/j.est.2018.11.013>
- Li, H., Cui, H., & Wan, Q. (2015). Distribution network reconfiguration based on second-order conic programming considering EV charging strategy. *Zhongguo Dianji Gongcheng Xuebao/Proceedings of the Chinese Society of Electrical Engineering*, 35(18), 4674–4681. <https://doi.org/10.13334/j.0258-8013.pcsee.2015.18.013>
- Meje, K. C., Bokopane, L., & Kusakana, K. (2020). Microgrids control strategies: A survey of available literature. *2020 8th International Conference on Smart Grid and Clean Energy Technologies, ICSGCE 2020, 2020*, 167–173. <https://doi.org/10.1109/ICSGCE49177.2020.9275651>
- Modarresi, J., Gholipour, E., & Khodabakhshian, A. (2016). A comprehensive review of the voltage stability indices. *Renewable and Sustainable Energy Reviews*, 63, 1–12. <https://doi.org/10.1016/j.rser.2016.05.010>
- Nguyen, T. T., Truong, A. V., & Phung, T. A. (2016). A novel method based on adaptive cuckoo search for optimal network reconfiguration and distributed generation allocation in distribution network. *International Journal of Electrical Power and Energy Systems*, 78, 801–815. <https://doi.org/10.1016/j.ijepes.2015.12.030>
- Nikitha, L., Anil, L., Tripathi, A., & Nagesh, S. (2018). Effect of electrical vehicle charging on power quality. *2017 International Conference on Energy, Communication, Data Analytics and Soft Computing, ICECDS 2017*, 2149–2153.

<https://doi.org/10.1109/ICECDS.2017.8389832>

- Pan, H., Ding, M., Chen, A., Bi, R., Sun, L., & Shi, S. (2018). Research on distributed power capacity and site optimization planning of AC/DC hybrid microgrids considering line factors. *Energies*, *11*(8), 1–18. <https://doi.org/10.3390/en11081930>
- Park, C. (2018). A Study of Smart Grid Effects on Electric Vehicle Management Considering the Change of the Power Capacity Mix. *The Open Transportation Journal*, *12*(1), 215–229. <https://doi.org/10.2174/1874447801812010215>
- Rahman, S., Khan, I. A., Khan, A. A., Mallik, A., & Nadeem, M. F. (2022). Comprehensive review & impact analysis of integrating projected electric vehicle charging load to the existing low voltage distribution system. *Renewable and Sustainable Energy Reviews*, *153*(October 2021), 111756. <https://doi.org/10.1016/j.rser.2021.111756>
- Ranjan, R., Venkatesh, B., & Das, D. (2003). Voltage stability analysis of radial distribution networks. *Electric Power Components and Systems*, *31*(5), 501–511. <https://doi.org/10.1080/15325000390127011>
- Rashid, M. H., & Tao, L. (2018). Parallel Combinatorial Optimization Heuristics with GPUs. *Proceedings - 2017 International Symposium on Computer Science and Intelligent Controls, ISCSIC 2017, 2018-Febru*, 118–123. <https://doi.org/10.1109/ISCSIC.2017.38>
- Reddy, M. S. K., Panigrahy, A. K., & Selvajothi, K. (2021). Minimization of Electric Vehicle charging Stations influence on Unbalanced radial distribution system with Optimal Reconfiguration using Particle Swarm Optimization. *2021 International Conference on Sustainable Energy and Future Electric Transportation, SeFet 2021*. <https://doi.org/10.1109/SeFet48154.2021.9375665>
- Reddy, M. S. K., & Selvajothi, K. (2020). Mitigation on the impact of electric vehicle charging stations in the radial distribution system. *4th IEEE Conference on Information and Communication Technology, CICT 2020*.

<https://doi.org/10.1109/CICT51604.2020.9312069>

- Sambaiah, K. S., & Jayabarathi, T. (2020). Loss minimization techniques for optimal operation and planning of distribution systems: A review of different methodologies. In *International Transactions on Electrical Energy Systems* (Vol. 30, Issue 2). <https://doi.org/10.1002/2050-7038.12230>
- Sehar, F., Pipattanasomporn, M., & Rahman, S. (2017). Demand management to mitigate impacts of plug-in electric vehicle fast charge in buildings with renewables. *Energy*, *120*(571), 642–651. <https://doi.org/10.1016/j.energy.2016.11.118>
- Triviño, A., González-González, J. M., & Aguado, J. A. (2021). Wireless power transfer technologies applied to electric vehicles: A review. *Energies*, *14*(6). <https://doi.org/10.3390/en14061547>
- Ul-Haq, A., Cecati, C., Strunz, K., & Abbasi, E. (2015). Impact of Electric Vehicle Charging on Voltage Unbalance in an Urban Distribution Network. *Intelligent Industrial Systems*, *1*(1), 51–60. <https://doi.org/10.1007/s40903-015-0005-x>
- Ülker, E. D., & Ülker, S. (2018). Enhanced leader particle swarm optimization for microwave matching networks. *Proceedings - 9th International Conference on Computational Intelligence and Communication Networks, CICN 2017, 2018-Janua*, 20–23. <https://doi.org/10.1109/CICN.2017.8319348>
- Uniyal, A., & Kumar, A. (2016). Comparison of optimal DG placement using CSA, GSA, PSO and GA for minimum real power loss in radial distribution system. *2016 IEEE 6th International Conference on Power Systems, ICPS 2016*, 1–6. <https://doi.org/10.1109/ICPES.2016.7584027>
- Wan Izzat Aiman Wan Abdul Manan, Azrin Saedi, Mohamad Heerwan Peeie, & Mohd Shahrin Abu Hanifah. (2021). Modeling of the Network Reconfiguration Considering Electric Vehicle Charging Load. *Proceedings of the 8th International Conference on Computer and Communication Engineering, ICCCE 2021, 2020*, 82–86.

<https://doi.org/10.1109/ICCCE50029.2021.9467143>

- Wang, J., Di, F., Meng, H., Meng, M., Luo, X., & Wang, Y. (2022). Coordinated Distribution Reconfiguration with Maintenance Scheduling Considering Electric Vehicles Charging Uncertainty. *2022 IEEE 5th International Electrical and Energy Conference (CIEEC)*, 168–173. <https://doi.org/10.1109/CIEEC54735.2022.9846071>
- Wang, L., Qin, Z., Slangen, T., Bauer, P., & van Wijk, T. (2021). Grid Impact of Electric Vehicle Fast Charging Stations: Trends, Standards, Issues and Mitigation Measures - An Overview. *IEEE Open Journal of Power Electronics*, 2(February), 56–74. <https://doi.org/10.1109/ojpel.2021.3054601>
- Wong, W. K., & Ming, C. I. (2019). A Review on Metaheuristic Algorithms: Recent Trends, Benchmarking and Applications. *2019 7th International Conference on Smart Computing and Communications, ICSCC 2019*. <https://doi.org/10.1109/ICSCC.2019.8843624>
- Xiaojing, Y., Qingju, J., & Xinke, L. (2019). Center particle swarm optimization algorithm. *Proceedings of 2019 IEEE 3rd Information Technology, Networking, Electronic and Automation Control Conference, ITNEC 2019, Itnec*, 2084–2087. <https://doi.org/10.1109/ITNEC.2019.8729510>
- Yang, X. S., & Deb, S. (2009). Cuckoo search via Lévy flights. *2009 World Congress on Nature and Biologically Inspired Computing, NABIC 2009 - Proceedings*, 210–214. <https://doi.org/10.1109/NABIC.2009.5393690>
- Yilmaz, M., & Krein, P. T. (2012). Review of charging power levels and infrastructure for plug-in electric and hybrid vehicles. *2012 IEEE International Electric Vehicle Conference*, 28(5), 1–8. <https://doi.org/10.1109/IEVC.2012.6183208>
- Yoldaş, Y., Önen, A., Muyeen, S. M., Vasilakos, A. V., & Alan, İ. (2017). Enhancing smart grid with microgrids: Challenges and opportunities. *Renewable and Sustainable Energy Reviews*, 72, 205–214. <https://doi.org/10.1016/j.rser.2017.01.064>

- Zaki Diab, A. A., Sultan, H. M., Mohamed, I. S., Kuznetsov Oleg, N., & Do, T. D. (2019). Application of different optimization algorithms for optimal sizing of pv/wind/diesel/battery storage stand-alone hybrid microgrid. *IEEE Access*, 7, 119223–119245. <https://doi.org/10.1109/ACCESS.2019.2936656>
- Zhang, Y., Song, X., Gao, F., & Li, J. (2016). Research of voltage stability analysis method in distribution power system with plug-in electric vehicle. *Asia-Pacific Power and Energy Engineering Conference, APPEEC, 2016-Decem(51177152)*, 1501–1507. <https://doi.org/10.1109/APPEEC.2016.7779740>
- Zhechao Li, Shaorong Wang, Jazebi, S., de Leon, F., & Wang, J. (2016). *Assessing the effect of system reconfiguration to enhance the capacity of electric-vehicle charging stations in radial distribution systems*. 1–5. <https://doi.org/10.1109/pesgm.2016.7741921>
- Zhou, B., Littler, T., & Meegahapola, L. (2016). Assessment of transient stability support for electric vehicle integration. *IEEE Power and Energy Society General Meeting, 2016-Novem*. <https://doi.org/10.1109/PESGM.2016.7741347>

AZRIN SAEDI

MSCIE

2022

IIUM

AZRIN SAEDI

MSCIE

2022

IIUM

AZRIN SAEDI

MSCIE

2022

IIUM